

行政院國家科學委員會專題研究計畫成果報告

國科會專題研究計畫成果報告撰寫格式說明

Preparation of NSC Project Reports

計畫編號：NSC 89-2215-E-009-112

執行期限：89年8月1日至90年8月31日

主持人：祁甦 國立交通大學光電工程研究所

計畫參與人員：曾弘毅，李健仲，呂英宗，蔣博文

國立交通大學光電工程研究所

張智明 上海交通大學應用物理學系

一、中文摘要

本計畫研究在摻有二階共振原子的非線性光纖光柵裡，光脈衝的存在機制與傳輸特性。針對此類摻有共振原子的光能隙結構，我們首度建立起完整的理論模型。研究更進一步發現，無損耗的光脈衝序列以及自感應透明—布拉格光固子皆可存在於這種摻有二階共振原子的非線性光纖光柵裡。

關鍵詞：光纖光柵、光能隙結構、布拉格光固子、自感應透明

Abstract

This project is devoted to the existence and physical mechanisms of optical pulses propagating in a nonlinear fiber grating doped uniformly with two-level atoms. For such a doped photonic bandgap structure, we establish a theoretical model for the first time. We further show that the distortionless pulse train and self-induced transparency soliton coexisting with Bragg soliton can propagate through the nonlinear fiber grating doped with resonant atoms.

Keywords: Fiber Grating, Photonic Bandgap Structure, Bragg soliton, Self-Induced Transparency

二、緣由與目的

The photonic bandgap (PBG) material has

been thoroughly investigated since Yablonovitch [1] introduced that such a periodic dielectric structure exhibits a forbidden band for optical energy. The simplest PBG structure is fiber Bragg grating, which has been widely applied in the practical lightwave communication systems. Although such a one-dimensional PBG material has a photon bandgap, the material nonlinearity can render the PBG “transparency” for nonlinear optical propagation. For example, gap solitons refer to solitary localization and solitary propagation of electromagnetic waves in a nonlinear PBG structure [2,3]. The central frequency of a gap soliton is inside the forbidden gap. On the basis of the nonlinear coupled-mode equations, Sipe and Winful first showed that a nonlinear PBG medium can support solitons of the nonlinear Schrödinger (NLS) equation [4]. Such a soliton is called a Bragg soliton [5-7,16]. Bragg solitons result from the material nonlinearity balancing with the quadratic grating dispersion. The central frequency of a Bragg soliton is outside the PBG but near the bandgap edge. Bragg solitons have been successfully observed in fiber Bragg gratings.

Another example of nonlinear optical pulse propagating through a bandgap material is the self-induced transparency (SIT) soliton in a doped PBG medium. The SIT results from the continuous absorption and reemission of electromagnetic radiation from the resonant atoms. The energy of resonant atoms periodically oscillating between the ground state and upper state leads to the

pulse-train propagation. Such coherent propagation is described by the Maxwell-Bloch equations, which have distortionless pulse-train solutions given by the Jacobi elliptic functions [8-10]. In particular, when the Jacobi elliptic modulus is unity, the pulse-train solution is reduced to a single-pulse solution of the hyperbolic secant function. This single pulse solution is called a SIT soliton. Both SIT solitons and periodic pulse trains have been experimentally observed in the materials without PBG structure. For the SIT in a PBG medium, Kozhokin and Kurizki [11-12] first showed that doping periodic thin layers of resonant atoms inside a nonlinear PBG structure can create a traveling “defect” in the forbidden band of this PBG structure. Hence a periodically doped PBG structure allows the SIT soliton propagating at the bandgap frequencies. Nevertheless, from a practical viewpoint, such a periodically doped PBG structure is difficult to realize. Therefore, Aközbek and John investigated the fundamental work on SIT solitary waves in PBG materials doped uniformly with resonant atoms [13]. However, the existence of the SIT analytic solution suitably for general frequency detuning and general phase modulation in a uniformly doped PBG medium has not been clarified, and even the SIT soliton with its central frequency being deep inside the forbidden gap have not yet been found.

In this project, we study the SIT in a uniformly doped PBG structure without using the slowly varying envelope approximation (SVEA). It is shown that the Maxwell-Bloch equations can be reduced to effective nonlinear coupled-mode equations (NLCMEs). Analytic distortionless pulse-train solutions and SIT-Bragg solitary solutions to these effective NLCMEs are obtained for the first time.

三、結果與討論

In this paper, we study the SIT in a nonlinear PBG structure doped uniformly with inhomogeneously broadening two-level atoms. It is shown that the Maxwell-Bloch

equations can be reduced to effective NLCME. An exact analytic pulse-train solution to these effective coupled-mode equations is obtained. Such a distortionless pulse-train solution is given by the sinusoidal function with a DC background and a modulated phase. In this project, we adopt the uniformly doped PBG model to study SIT pulse-train propagation. In contrast with Ref. [13], our model is more general than that in Ref. [13]: (i) In our uniformly doped PBG model, we derive the Maxwell-Bloch equation without using the slowly varying envelope approximation. The formation of the SIT effects require ultrashort pulses with their pulse widths being shorter than the relaxation times of the resonant atoms, but the SVEA is not valid for a ultrashort pulse. Thus we use the model without making the SVEA. Moreover, in Ref. [13], the authors emphasize that they have neglected the linear contribution to the dispersion relation arising from the two-level atoms. Hence the allowed concentration of dopant atoms are limited for their SVEA model. In Ref. [10], it has been found that SIT could induce an additional negative dispersion of which it has not been predicted by the SIT theory under SVEA. Since the Maxwell-Bloch equation without using the SVEA can reduce to Bloch-NLCMEs, these effective NLCMEs completely involve the SIT-induced negative dispersion and the effective grating dispersion. (ii) The phase functions of the forward and Bragg scattering field are assumed to be identical in Ref. [13]. On the contrary, we consider general phase functions. This general consideration of the phase functions result in the demonstration that the phase modulation effects of the forward and Bragg scattering field both satisfy the general SIT chirping equation. Notice that the Jacobi elliptic pulse-train solutions to the Maxwell-Bloch equations for a resonance medium without PBG structure have been theoretically studied [8-9]. However, our model involves considering a resonance medium whose resonant atoms embedded in a PBG structure. It is well known that a PBG structure has a forbidden band for optical energy, but the SIT provide a mechanism to

make it possible that an optical pulse train can pass through the PBG medium.

By using the multiple-scale analysis under the slow-velocity limit, the effective NLCMEs can be further reduced to an effective NLSE. The quadratic dispersion of this NLSE involves quadratic grating dispersion and the linear contribution from the resonant atoms; moreover, the nonlinearity of this NLSE includes the material Kerr-nonlinearity and resonant enhanced nonlinearity. The soliton solution to this NLSE indicates the coexistence of a SIT soliton and a Bragg soliton. Such a mixed state is called a SIT-Bragg soliton. Consequently, many of the results known for the NLS soliton and Bragg soliton can be easily applied to clarify the characteristics of a SIT-Bragg soliton. Furthermore, it is also shown that the SIT-Bragg soliton has to obey the general SIT phase modulation effect. Hence a SIT-Bragg soliton cannot exhibit chirping. The chirped SIT has to be a pulse train given by the Jacobi elliptic function or the above mentioned sinusoidal functions. It is found that even if the carrier frequency of the SIT soliton and SIT pulse train is deep inside the forbidden band, the optical pulse can propagate through the PBG structure and obey the general SIT phase modulation effect. Numerical examples of the SIT pulse train and the SIT-Bragg soliton in a PBG structure doped uniformly with Lorentzian line-shape two-level atoms are demonstrated [14-15]. Because both SIT and Bragg scattering slow down the light, the group velocity of the SIT in a doped PBG medium can be substantially less than the speed of light in a bare nonlinear medium.

四、計畫成果自評

The results of this project include

- (i) We establish the effective NLCMEs to model the SIT in a doped PBG structure. Consequently, many of the results known for the NLCMEs can be easily applied to clarify the existence of the SIT in a nonlinear doped PBG structure.
- (ii) Exact analytic pulse-train solutions to the effective NLCMEs are obtained.

(iii) A single pulse solution indicating the SIT-Bragg soliton is obtained.

(iv) We also show that the SIT effects in a doped PBG structure obey the general SIT chirping relation.

These results are all obtained for the first time. They explicitly describe the existence and physical mechanisms of optical pulses propagating in a nonlinear fiber grating doped uniformly with two-level atoms.

Since the PBG medium is transparent for the SIT, such research has attracted much interest. It has been suggested that a doped nonlinear PBG structure could be applied to high sensitivity optical filter, pulse reshaping, and optical switching devices for optical computing, optical interconnection and optical communication system [13]. It is our hope that our general model can accurately estimate the associated medium parameters and the initial condition of the input optical field for designing such a device. These subjects would lead to practical applications of uniformly doped PBG structures in the vast area of lightwave systems.

五、參考文獻

- [1] E. Yablonovitch, Phys. Rev. Lett. **58**, 2059 (1987).
- [2] A. B. Aceves and S. Wabnitz, Phys. Lett. A. **141**, 37 (1989).
- [3] C. M. de Sterke and J. E. Sipe, in *Progress in Optics*, E. Wolf, ed. (North-Holland, Amsterdam, 1994), Vol. XXXIII, Chap. III.
- [4] J. E. Sipe and H. G. Winful, Opt. Lett. **13**, 132 (1988).
- [5] B. J. Eggleton, C. M. de Sterke and R. E. Slusher, J. Opt. Soc. Am. B, **14**, 2980 (1997).
- [6] B. J. Eggleton, C. M. de Sterke and R. E. Slusher, J. Opt. Soc. Am. B, **16**, 587 (1999).
- [7] B. J. Eggleton, R. E. Slusher, C. M. de Sterke, P. A. Krug and J. E. Sipe, Phys. Rev. Lett, **76**, 1627 (1996).
- [8] J. H. Eberly, Phys. Rev. Lett. **22**, 720 (1969).
- [9] L. Matulic and J. H. Eberly, Phys. Rev. A. **6**, 822 (1972).
- [10] S. Chi, T. Y. Wang and S. Wen, Phys. Rev. A. **47**, 3371 (1993).
- [11] A. E. Kozhokin and G. Kurizki, Phys. Rev. Lett. **74**, 5020 (1995).
- [12] A. E. Kozhokin, G. Kurizki and B. A. Malomed, Phys. Rev. Lett. **81**, 3647 (1998).
- [13] N. Aközbebek and S. John, Phys. Rev. E. **58**, 3876 (1998).
- [14] 祁姓, 曾弘毅: 附件一(投稿於 Phys. Rev. Lett.).
- [15] 祁姓, 曾弘毅: 附件二(投稿於 Phys. Rev. E).
- [16] 祁姓, 羅博仁, 曾弘毅: 附件三 (投稿於 Optics Communications).

Coexistence of Self-induced Transparency Soliton and Bragg Soliton

Sien Chi and Hong-Yih Tseng

Institute of Electro-Optical Engineering, National Chiao-Tung University, Hsinchu, Taiwan, 300, R.O.C

We show that a nonlinear photonic bandgap medium doped uniformly with inhomogeneously broadening two-level atoms can support solitons of the nonlinear Schrödinger equation. Such a self-induced transparency (SIT) soliton can propagate through the nonlinear doped PBG medium even if its central frequency is deep inside the forbidden band. The physical mechanisms of a SIT soliton deep inside the gap are presented and numerically studied.

Gap solitons refer to solitary localization and solitary propagation of electromagnetic waves in a nonlinear photonic bandgap (PBG) structure [1,2]. The central frequency of a gap soliton is inside the forbidden gap. On the basis of the nonlinear coupled-mode equations, Sipe and Winful first showed that a nonlinear PBG medium can support solitons of the nonlinear Schrödinger (NLS) equation [3]. Such a soliton is called a Bragg soliton [4-6]. Bragg solitons result from the material nonlinearity balancing with the quadratic grating dispersion. The central frequency of a Bragg soliton is outside the PBG but near the bandgap edge. Bragg solitons have been successfully observed in fiber Bragg gratings. The experimental results agree well with the NLS model.

More recently, the self-induced transparency (SIT) soliton in a nonlinear PBG structure doped with resonant atoms has drawn considerable attention [7-9]. SIT solitons are coherent optical pulses propagating through resonant medium without loss and distortion. Such coherent propagation is described by the Maxwell-Bloch equations [10-12]. For the SIT in a *uniformly* doped nonlinear PBG structure, Aközbeke and John investigated the fundamental work on soliton solutions for frequency detuned *near the PBG edge* and called them SIT-gap solitons [9]. Because the dopant density and the atomic detuning frequency dramatically change the characteristics of a SIT-gap soliton, it has been suggested that applying such solitary propagation may be very useful in optical telecommunications and optical computing. However, the physical mechanisms of a SIT soliton with its central frequency being *deep inside the forbidden gap* have not yet been clarified, and even its existence has not been proven.

In this letter, we show that a NLS soliton deep inside the bandgap can exist in a uniformly doped nonlinear PBG medium. Such a soliton is called a SIT-Bragg soliton. Numerical examples of the SIT-Bragg solitons in an As_2S_3 -based PBG structure doped uniformly with Lorentzian line-shape two-level atoms are presented.

We consider a one-dimensional Bragg grating formed in a host medium with Kerr nonlinearity. The periodic variations of the refractive index inside the grating region is

$$\tilde{n}(\omega) = n(\omega) + n_2 |E|^2 + n_a \cos(2\beta_g z), \quad (1)$$

where E is the electric field in the medium, $n(\omega)$ is the frequency-dependent refractive index, n_2 is the Kerr nonlinear-index coefficient, n_a is the magnitude of the periodic index variations, and β_g is the grating wave

number. The two-level atoms with the resonant frequency ω_r are uniformly embedded in this Kerr host medium. From Maxwell's equations, the wave equation describing light propagation in such a medium is

$$\nabla^2 E - \frac{1}{c^2} \frac{\partial^2 E}{\partial t^2} - \mu_0 \frac{\partial^2 P}{\partial t^2} = \mu_0 \frac{\partial^2 P_r}{\partial t^2}, \quad (2)$$

where c is the velocity of light in vacuum, μ_0 is the vacuum permeability, P is the electric induced polarization including the linear and nonlinear contributions of the host medium, and P_r is the resonant polarization due to the two-level atoms. In Fourier domain, Eq. (2) becomes

$$\nabla^2 \tilde{E} + \tilde{n}(\omega)^2 \frac{\omega^2}{c^2} \tilde{E} = -\mu_0 \omega^2 \tilde{P}_r, \quad (3)$$

where \tilde{E} is the Fourier transform of E , and \tilde{P}_r is the Fourier transform of P_r . The electric field E propagating along the z direction in such a doped nonlinear PBG structure can be expressed as

$$E(z, t) = \frac{1}{2} [E_+(z, t) e^{i(\beta_g z - \omega_B t)} + E_-(z, t) e^{i(-\beta_g z - \omega_B t)}] + c.c., \quad (4)$$

where $c.c.$ stands for complex conjugate, E_+ and E_- are forward and Bragg scattering envelopes, and ω_B is the Bragg frequency. In addition, the macroscopic polarization caused by the dopants is written as

$$P_r(z, t) = \frac{1}{2} [P_+(z, t) e^{i(\beta_g z - \omega_B t)} + P_-(z, t) e^{i(-\beta_g z - \omega_B t)}] + c.c., \quad (5)$$

where P_+ and P_- correspond to the polarization envelopes induced by E_+ and E_- , respectively. Substituting Eqs. (1), (4) and (5) into Eq. (3), and then taking the inverse Fourier transform under the assumptions of $n_2 \ll n$ and $n_a \ll n$, we obtain

$$\begin{aligned} & \pm i \frac{\partial E_{\pm}}{\partial z} + i\beta_1 \frac{\partial E_{\pm}}{\partial t} + \delta\beta_0 E_{\pm} + \kappa E_{\mp} \\ & + \Gamma(|E_{\pm}|^2 + 2|E_{\mp}|^2) E_{\pm} + \frac{\mu_0 \omega_B^2}{2\beta_0} (P_{\pm} + \frac{2i}{\omega_B} \frac{\partial P_{\pm}}{\partial t}) = 0, \end{aligned} \quad (6)$$

where β_j ($j=0,1$) are determined by the mode-propagation constant $\beta(\omega) \equiv (\omega/c)n(\omega)$ via $\beta_j = d^j \beta / d\omega^j \Big|_{\omega=\omega_B}$,

$\kappa = \pi n_a / \lambda$ is the coupling coefficient of the periodic structure, Γ denotes the nonlinearity coefficient, and $\delta\beta_0 = \beta_0 - \beta_g$ implies the wave number detuning from the exact Bragg resonance. Notice that in contrast with the wave equations adopted in Ref. [9], we take into account the first-order time derivatives of the polarization envelopes. We will show that these terms enable our model to involve the linear contribution to the dispersion relation arising from the resonant atoms.

We now consider the atomic Bloch equations. The complex envelopes E_{\pm} and P_{\pm} are further written as

$$E_{\pm}(z, t) = a_{\pm}(z, t) \exp[i\varphi_{\pm}(z, t)], \quad (7a)$$

$$P_{\pm}(z, t) = [U_{\pm}(z, t) + iV_{\pm}(z, t)] \exp[i\varphi_{\pm}(z, t)], \quad (7b)$$

where a_{\pm} are real envelopes, φ_{\pm} are phase functions, U_{\pm} correspond to the dispersion (in phase) induced by the resonant atoms, and V_{\pm} correspond to the absorption (in quadrature) caused by the resonant atoms. Moreover, the Bloch vectors (u_{\pm}, v_{\pm}, w) relate the macroscopic polarization and population difference as follows:

$$(U_{\pm}, V_{\pm}, W) = \int_{-\infty}^{\infty} (u_{\pm}, v_{\pm}, w) g(\Delta\omega - \Delta\omega_{r0}) d(\Delta\omega), \quad (8)$$

where $\Delta\omega$ is defined by $\Delta\omega = \omega_r - \omega_b$, (u_{\pm}, v_{\pm}, w) describe the components of the polarization and population difference contributed from the atoms with resonant frequencies in the whole range of $\Delta\omega$, $g(\Delta\omega - \Delta\omega_{r0})$ is the normalized inhomogeneous-broadening line-shape function, $\Delta\omega_{r0}$ is defined by $\Delta\omega_{r0} = \omega_{r0} - \omega_b$, and ω_{r0} is the center of the broadening line-shape function. Here, the quantity $W = \mu(N_1 - N_2)$ is the macroscopic population difference multiplied by the transition matrix element μ between the ground state (N_1) and upper state (N_2) of the two-level system. Furthermore, to keep a closed set of the Bloch equations, we assume $\varphi_{\pm}(z, t) = \phi(z, t) \pm \psi(z, t)$ and $w = w_0 + 2w_1 \cos[2\psi(z, t) + 2\beta_g z]$. After neglecting the atomic relaxation times and the terms oscillating as $\exp(\pm i3\beta_g z)$, we express the atomic Bloch equations as

$$\frac{\partial u_{\pm}}{\partial t} = (\Delta\omega + \frac{\partial\varphi_{\pm}}{\partial t}) v_{\pm}, \quad (9a)$$

$$\frac{\partial v_{\pm}}{\partial t} = -(\Delta\omega + \frac{\partial\varphi_{\pm}}{\partial t}) u_{\pm} + \frac{\mu}{\hbar} (a_{\pm} w_0 + a_{\mp} w_1), \quad (9b)$$

$$\frac{\partial w_0}{\partial t} = -\frac{\mu}{\hbar} (a_{+} v_{+} + a_{-} v_{-}), \quad (9c)$$

$$\frac{\partial w_1}{\partial t} = -\frac{\mu}{2\hbar} (a_{+} v_{-} + a_{-} v_{+}). \quad (9d)$$

The atomic Bloch equations can be solved by using the the

factorization ansatz $v_{\pm}(\Delta\omega, z, t) = v_{\pm}(0, z, t) f(\Delta\omega)$, where $f(\Delta\omega) = (1 + c_1 \Delta\omega + c_2 \Delta\omega^2)^{-1}$ is the dipole spectral-response function of the resonant atoms. Leading to a self-consistent solution to the Maxwell-Bloch equations, such an ansatz has been widely applied to solve the SIT problems. The undetermined constants c_1 and c_2 both relate to the frequency detuning and the pulse width of the electric field, and they will be identified in the next section. Using this factorization ansatz, we have⁹⁻¹²

$$u_{\pm} = [c_1 - (\frac{\partial\varphi_{\pm}}{\partial t} - \Delta\omega)c_2] \frac{\mu}{\hbar} w_i f(\Delta\omega) a_{\pm}(z, t), \quad (10a)$$

$$v_{\pm} = c_2 \frac{\mu}{\hbar} w_i f(\Delta\omega) \frac{\partial}{\partial t} a_{\pm}(z, t), \quad (10b)$$

$$w_0 = w_i - \frac{c_2}{2} (\frac{\mu}{\hbar})^2 w_i f(\Delta\omega) [a_{+}^2(z, t) + a_{-}^2(z, t)], \quad (10c)$$

$$w_1 = -\frac{c_2}{2} (\frac{\mu}{\hbar})^2 w_i f(\Delta\omega) [a_{+}(z, t) a_{-}(z, t)], \quad (10d)$$

where w_i is the initial population difference multiplied by μ and it is assumed in the ground state of the two-level system, i.e., $w_i = N_D \mu$, where $N_D = N_1 + N_2$ is the doping concentration of the resonant atoms. Substituting Eqs. (10) into Eqs. (9a) and (9b), we obtain

$$2 \frac{\partial a_{\pm}}{\partial t} \frac{\partial\varphi_{\pm}}{\partial t} + \frac{\partial^2\varphi_{\pm}}{\partial t^2} a_{\pm} = \frac{c_1}{c_2} \frac{\partial a_{\pm}}{\partial t}, \quad (11a)$$

$$\frac{\partial^2 a_{\pm}}{\partial t^2} = [\frac{1}{c_2} - \frac{c_1}{c_2} (\frac{\partial\varphi_{\pm}}{\partial t}) + (\frac{\partial\varphi_{\pm}}{\partial t})^2] a_{\pm} - \frac{\mu^2}{2\hbar^2} (a_{\pm}^2 + 2a_{\mp}^2) a_{\pm}. \quad (11b)$$

Defining $s = \mu_0 \omega_b^2 w_i \mu / (2\beta_g \hbar)$, $I_1 = \int_{-\infty}^{\infty} f(\Delta\omega) g(\Delta\omega - \Delta\omega_{r0}) d(\Delta\omega)$, and $I_2 = \int_{-\infty}^{\infty} \Delta\omega f(\Delta\omega) g(\Delta\omega - \Delta\omega_{r0}) d(\Delta\omega)$, and substituting Eqs. (7), (8), (10) and (11) into Eqs. (6), we obtain

$$\pm i \frac{\partial E_{\pm}}{\partial z} + i\beta_1^e \frac{\partial E_{\pm}}{\partial t} + \delta\beta_e E_{\pm} + \kappa E_{\mp} + \Gamma_e (|E_{\pm}|^2 + 2|E_{\mp}|^2) E_{\pm} = 0, \quad (12)$$

where the effective parameters are $\delta\beta_e = \delta\beta_0 + sc_1 I_1 - 2sI_1 / \omega_b + sc_2 I_2$, $\beta_1^e = \beta_1 + sc_2 I_1 + 2sc_2 I_2 / \omega_b$, and $\Gamma_e = \Gamma + sc_2 I_1 \mu^2 / (\omega_b \hbar^2)$. As a result, Eqs. (6) are reduced to effective nonlinear coupled-mode equations (NLCMEs). The effective NLCMEs describe that pulse propagation through a uniformly doped PBG structure is equivalent to that through an effective PBG structure without dopants. Consequently, many of the results known for the NLCMEs can be easily applied to clarify the existence of the SIT soliton in a nonlinear doped PBG structure.

The linear terms of the effective NLCMEs are considered first. Their dispersion relation is written as $\Omega = \omega - \omega'_b = \pm \sqrt{Q^2 + \kappa^2} / \beta_1^e \equiv \Omega_{\pm}$, where the equivalent

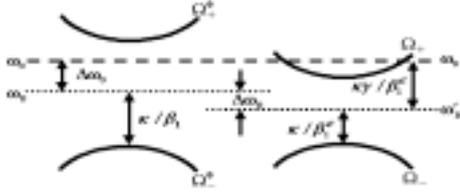


Fig.1. Frequency detuning of E_{\pm} with respect to the original dispersion relation Ω_{\pm}^0 of the PBG structure and the effective dispersion relation Ω_{\pm} for the linear terms of Eqs. (12).

Bragg frequency has been shifted to $\omega'_B = \omega_B - (-\delta\beta_e / \beta_1^e)$ because of the resonant atoms; likewise Ω and Q are the frequency and wave number detuning from the effective Bragg resonance, respectively. Here we define $\Delta\omega_B = -\delta\beta_e / \beta_1^e$ and $\Delta\omega_0 = \omega_0 - \omega_B$, where ω_0 is the input carrier frequency of the electric field. Figure 1 schematically shows the frequency detuning $\Delta\omega_0$ with respect to the dispersion relations. The hyperbolic curves Ω_{\pm}^0 indicate the original dispersion relation of the PBG structure without dopants, and Ω_{\pm} indicate the effective dispersion relation associated with the linear terms of Eqs. (12), i.e., Ω_{\pm}^0 are identical to $\Omega_{\pm}|_{N_D=0}$. The center of the original forbidden gap is located at ω_B , and this original gap has a width being equal to $2\kappa / \beta_1$. After we take into account the effects from the resonant atoms, not only the Bragg frequency is shifted to ω'_B , but also the width of this effective gap is narrowed to $2\kappa / \beta_1^e$. Note that Ω_{\pm} indicate that the dispersion relation provides upper and lower frequency branches. The Bloch waves (linear eigenstates) corresponding to these two branches are exact solutions to the linear terms of Eqs. (12). In addition, the group velocity of the Bloch wave on the upper branch is $v_g = \partial\Omega_+ / \partial Q$; thus we have $\Omega_+ = \kappa\gamma / \beta_1^e$ and $Q = v\kappa\gamma$ by defining $v = \beta_1^e v_g$ and $\gamma = 1 / \sqrt{1 - v^2}$. The solution to Eqs. (12) now can be regarded as the envelope function of the Bloch wave corresponding to the upper bandgap edge. Such an envelope function expressed as $E(z, t)$ describes how the positive nonlinearity weakly modulates the Bloch wave. Consequently, under the limitations of slow-velocity ($v \ll 1$), the effective NLCMEs for $E_{\pm}(\xi, \tau) \approx \pm E(\xi, \tau) \exp[i(Qz - \Omega_{\pm}t)] / \sqrt{2}$ can be well approximated by an effective NLS equation

$$i \frac{\partial E}{\partial \xi} - \frac{1}{2} \beta_2^e \frac{\partial^2 E}{\partial \tau^2} + \Gamma_v |E|^2 E = 0, \quad (13)$$

where $\tau = t - z / v_g$ and $\xi = z$ are the moving frame coordinates, and the parameters of this NLSE depend on the effective undoped PBG structure via⁵

$$\Gamma_v = \frac{3 - v^2}{2v} \Gamma_e, \quad \beta_2^e = -(\beta_1^e)^2 \frac{1}{\kappa\gamma^3 v^3}. \quad (14)$$

Although the NLSE has well-known soliton solutions, it is

noticed that the solution to Eq. (13) has to satisfy Eqs. (11). We seek the solution in the form of

$$E(\xi, \tau) = a(\tau) \exp[i\varphi(\tau) + i\xi / (2L_D)], \quad (15)$$

where L_D is the dispersion length representing the length scale over which the dispersive effects are important. Integrating Eqs. (11a) and using $a_{\pm}(z, t) = \pm |E(\xi, \tau)| / \sqrt{2} = \pm a(\tau) / \sqrt{2}$, we obtain

$$\frac{\partial \varphi_+}{\partial \tau} = \frac{\partial \varphi_-}{\partial \tau} = \frac{c_1}{2c_2} + \frac{2c_0}{a(\tau)^2}, \quad (16)$$

where c_0 is an integration constant, and we have $\Delta\omega_0 = -\Delta\omega_B + \Omega_{\pm} = -c_1 / (2c_2)$ and $\partial\varphi / \partial\tau = 2c_0 / a(\tau)^2$. Eq. (16) describes the general phase modulation, or pulse chirping in the SIT. The constant $-c_1 / (2c_2)$ indicates that the carrier frequency of the optical field is $\omega_B - c_1 / (2c_2)$; moreover, the instantaneous frequency is inversely proportional to the pulse intensity. Such a chirping relation has been studied for the SIT in a nonlinear medium *without PBG structure*. Substituting Eq. (16) and $a_{\pm}(z, t) = \pm a(\tau) / \sqrt{2}$ into Eqs. (11b), and then substituting Eq. (15) and $\partial\varphi / \partial\tau = 2c_0 / a(\tau)^2$ into Eq. (13), we find that both of the resulting equations lead to

$$\frac{\partial^2 a}{\partial \tau^2} = \frac{4c_0^2}{a^3} + \gamma_1 a + \gamma_3 a^3, \quad (17)$$

where

$$\gamma_1 \equiv \frac{1}{c_2} - \frac{c_1^2}{4c_2^2} = \frac{1}{|\beta_2^e| L_D}, \quad \gamma_3 \equiv \frac{3\mu^2}{4\hbar^2} = \frac{2\Gamma_v}{|\beta_2^e|}. \quad (18)$$

For $c_0 \neq 0$, Eq. (17) has a distortionless pulse-train solution given by the Jacobi elliptic function. Such pulse-train propagation results from the energy of resonant atoms periodically oscillating between the ground state and upper state. Here we focus our attention on a single-pulse solution to Eq. (17). For $c_0 = 0$, we obtain $a(\tau) = A_0 \operatorname{sech}(\tau / T_0)$, where $A_0 = \sqrt{|\beta_2^e| / (\Gamma_v T_0^2)}$ $= 2\sqrt{2}\hbar / (\sqrt{3}\mu T_0)$ is the pulse amplitude, and $T_0 = 1 / \sqrt{\gamma_3}$ is the pulse width. Consequently, we obtain

$$E_{\pm}(\xi, \tau) = \pm \frac{A_0}{\sqrt{2}} \operatorname{sech}\left(\frac{\tau}{T_0}\right) e^{i[\xi / (2L_D) + Qz - (-\Delta\omega_B + \Omega_{\pm})t]}, \quad (19)$$

where the dispersion length is $L_D = T_0^2 / |\beta_2^e|$. Because the central frequency $\omega_0 = \omega_B - \Delta\omega_B + \Omega_{\pm}$ of this optical field is inherently located at the effective bandgap edge, Eqs. (19) express a Bragg soliton. This soliton undergoes the effective nonlinearity and quadratic grating dispersion expressed in Eqs. (14). Furthermore, such a soliton solution also satisfies

the atomic Bloch equations. Hence it indicates the coexistence of a SIT soliton and a Bragg soliton. This mixed state is referred to as a SIT-Bragg soliton. Notice that the effective PBG structure described by Eqs. (12) is not fixed by the associated medium parameters. Such an effective model can be determined by the input pulse width T_0 incorporated with either the atomic frequency detuning $\Delta\omega_{r_0}$ or the Bragg frequency detuning $\Delta\omega_0$. Therefore, a SIT-Bragg soliton can exist deep inside the original forbidden gap as long as $\Delta\omega_0 = -c_1/(2c_2) < \kappa/\beta_1$ (see Fig. 1).

To examine the existence of a SIT-Bragg soliton, we numerically study an As_2S_3 -based fiber Bragg grating (As_2S_3 -FBG) doped uniformly with Lorentzian line-shape two-level atoms. The As_2S_3 -based fiber is a type of chalcogenide-glass fiber with the Kerr nonlinearity being two orders of magnitude higher than the value of silica-glass fiber. Because of its high nonlinearity, As_2S_3 -based fiber has been widely investigated for all-optical switching. Moreover, the fabrication of an As_2S_3 -FBG has been reported. The material parameters for such an As_2S_3 -FBG are assumed to be $n(\omega_0) = 2.39$, $\beta_0 = 5.9 \times 10^6 \text{ m}^{-1}$, $\beta_1 = 7.9 \times 10^9 \text{ s/m}$, and $n_2 = 2.5 \times 10^{-20} \text{ m}^2/V^2$ at 1550 nm wavelength region. The coupling coefficient of the Bragg grating is $\kappa = 100 \text{ cm}^{-1}$ corresponding to the index vibration $n_a = 0.005$ at the Bragg wavelength $\lambda_b = 1553 \text{ nm}$. In contrast with κ describing the coupling strength, we use $\delta\beta_0 = \beta_1\Delta\omega_0$ to indicate the carrier detuning and define $\delta\beta_r = \beta_1\Delta\omega_{r_0}$ to express the atomic detuning from the exact Bragg resonance. For the embedded resonant atoms, the Lorentzian line-shape function is written as $g(\Delta\omega - \Delta\omega_{r_0}) = (\Delta\omega_a/2\pi) / [(\Delta\omega - \Delta\omega_{r_0})^2 + (\Delta\omega_a/2)^2]$, where $\Delta\omega_a = 2\pi\Delta f_a$ is the full width at half maximum (FWHM) of $g(\Delta\omega - \Delta\omega_{r_0})$. In addition, we assume that $\Delta f_a = 1472 \text{ GHz}$, $\mu = 1.4 \times 10^{-32} \text{ C} \cdot \text{m}$, and $N_D = 8.0 \times 10^{24} \text{ m}^{-3}$. Note that the large Δf_a is realistic for Erbium atoms. By using Eqs. (18) and $\Delta\omega_0 = -\Delta\omega_B + \Omega_+ = -c_1/(2c_2)$ under the assumptions of $\Delta\omega_a \gg 1/T_0$, Fig. 2(a) shows the FWHM $T_w \approx 1.763T_0$ of the SIT-Bragg solitons as functions of $\delta\beta_r$ at $\delta\beta_0 = 20 \text{ cm}^{-1}$ (dotted line), $\delta\beta_0 = 22 \text{ cm}^{-1}$ (dashed line), and $\delta\beta_0 = 24 \text{ cm}^{-1}$ (solid line). The FWHM curve for a fixed $\delta\beta_0$ is symmetric to $\delta\beta_r = \delta\beta_0$; namely the minimum T_w occurs on exact atomic resonance $\omega_0 = \omega_{r_0}$. Moreover, detuning the atomic transition frequency from the exact atomic resonance slightly increases the required FWHM for a SIT-Bragg soliton. By contrast, detuning the carrier frequency from the exact Bragg resonance significantly increases the required T_w . Fig. 2(b) shows the required FWHM (solid curve) and the corresponding peak intensity (dotted curve) for a SIT-Bragg soliton at $\delta\beta_r = 0$ as functions of $\delta\beta_0$. Obviously, a larger Bragg detuning implies higher peak intensity for the existence of a SIT-Bragg soliton. The required peak

intensity for the SIT-Bragg soliton in this doped As_2S_3 -FBG is one order of magnitude lower than the value for a Bragg soliton in silica-FBG. The group velocities in the range $20 < \delta\beta_0 < 100$ almost maintain a constant $v_g = 1.31 \times 10^6 \text{ m/s}$, which is dominated by the nonlinearity coefficient and the atomic doping concentration. This quantity of v_g results in $v \approx 0.025$ and corresponds to $1/250$ of the speed of light in vacuum. Note that Fig. 2 (b) does not exhibit the FWHM and peak intensity for $0 < \delta\beta_0 < 20$, because the required FWHM for this range dramatically exceeds 1000 ps that is not much less than the atomic relaxation times. From an experimental viewpoint, the atomic relaxation processes would incoherently absorb the pulse energy for $0 < \delta\beta_0 < 20$. Finally, in such a doped As_2S_3 -FBG the SIT-Bragg soliton cannot exist for $\delta\beta_0 < 0$. The existence of a SIT-Bragg soliton for $\delta\beta_0 < 0$ could be clarified by deriving the similar effective NLSE to describe how the negative nonlinearity modulates the Bloch wave on the lower effective bandgap edge.

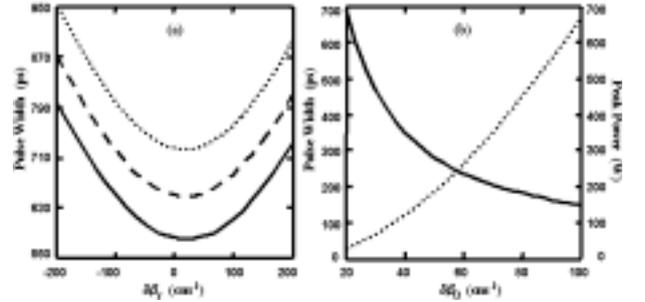


Fig. 2. (a) FWHM of the SIT-Bragg solitons as functions of $\delta\beta_r$ at $\delta\beta_0 = 20 \text{ cm}^{-1}$ (dotted line), $\delta\beta_0 = 22 \text{ cm}^{-1}$ (dashed line), and $\delta\beta_0 = 24 \text{ cm}^{-1}$ (solid line). (b) FWHM (solid curve) and the corresponding peak intensity (dotted curve) for a SIT-Bragg soliton at $\delta\beta_r = 0$ as functions of $\delta\beta_0$. Note that the original bandgap edge is located at $\delta\beta_0 = \pm\kappa = \pm 100 \text{ cm}^{-1}$.

In summary, we have derived the effective NLSE to model the SIT effect in a nonlinear PBG structure doped uniformly with inhomogeneously broadening two-level atoms. According to the effective NLSE, we show that SIT solitons can coexist with Bragg solitons. Such a mixed state is called a SIT-Bragg soliton. A SIT-Bragg can propagate through a nonlinear doped PBG medium, even if the central frequency of the SIT-Bragg soliton is deep inside the forbidden gap. The input pulse width in conjunction with the Bragg frequency detuning and atomic frequency detuning strictly constrains the existence of a SIT-Bragg soliton. Furthermore, the material nonlinearity and atomic doping concentration determine the slow-light property of such a soliton. Hence we suggest that the mechanisms of a SIT-Bragg soliton could be applied to study the sensitively tunable filter, high-speed optical switch, and all-optical delay line in the vast area of lightwave systems.

This work was supported by the National Science Council, Taiwan, R.O.C. under contract NSC 89-2215-E-009-112.

References

1. A. B. Aceves and S. Wabnitz, *Phys. Lett. A* **141**, 37 (1989).
2. C. M. de Sterke and J. E. Sipe, in *Progress in Optics*, E. Wolf, ed. (North-Holland, Amsterdam, 1994), Vol. XXXIII, Chap. III.
3. J. E. Sipe and H. G. Winful, *Opt. Lett.* **13**, 132 (1988).
4. B. J. Eggleton, C. M. de Sterke and R. E. Slusher, *J. Opt. Soc. Am. B*, **14**, 2980 (1997).
5. B. J. Eggleton, C. M. de Sterke and R. E. Slusher, *J. Opt. Soc. Am. B*, **16**, 587 (1999).
6. B. J. Eggleton, R. E. Slusher, C. M. de Sterke, P. A. Krug and J. E. Sipe, *Phys. Rev. Lett.* **76**, 1627 (1996).
7. A. E. Kozhekin and G. Kurizki, *Phys. Rev. Lett.* **74**, 5020 (1995).
8. A. E. Kozhekin, G. Kurizki and B. A. Malomed, *Phys. Rev. Lett.* **81**, 3647 (1998).
9. N. Aközbek and S. John, *Phys. Rev. E* **58**, 3876 (1998).
10. J. H. Eberly, *Phys. Rev. Lett.* **22**, 720 (1969).
11. L. Matulic and J. H. Eberly, *Phys. Rev. A* **6**, 822 (1972).
12. S. Chi, T. Y. Wang and S. Wen, *Phys. Rev. A* **47**, 3371 (1993).
13. G. P. Agrawal, *Applications of Nonlinear Fiber Optics* (Academic Press, New York, 2001).

Distortionless pulse-train propagation in a nonlinear photonic bandgap structure doped uniformly with inhomogeneously broadening two-level atoms

Sien Chi and Hong-Yih Tseng

Institute of Electro-Optical Engineering, National Chiao-Tung University, Hsinchu, Taiwan, 300, R.O.C

We have studied the self-induced transparency (SIT) pulse train in a one-dimensional nonlinear photonic bandgap (PBG) structure doped uniformly with inhomogeneously broadening two-level atoms. The Maxwell-Bloch equations describing pulse propagation through such a uniformly doped PBG structure are derived without using the slowly varying envelope approximation. It is shown that the Maxwell-Bloch equations can be reduced to effective nonlinear coupled-mode equations. An exact analytic pulse-train solution to these effective coupled-mode equations is obtained. Such a distortionless pulse-train solution is given by sinusoidal functions and has to exist with background intensity. We also show that the pulse train propagating in a uniformly doped nonlinear PBG structure obeys the general SIT phase modulation effect. Furthermore, because both SIT and Bragg scattering slow down the light, the pulse-train group velocity can be substantially less than the speed of light in a bare nonlinear medium. Numerical examples of the SIT pulse train in a silica-based PBG structure doped uniformly with Lorentzian line-shape two-level atoms are demonstrated.

I. INTRODUCTION

The distortionless propagation of light through an optical resonance medium has been widely discussed since McCall and Hahn discovered self-induced transparency (SIT) [1]. The SIT is characterized by the continuous absorption and reemission of electromagnetic radiation from the resonant atoms. When the coherent interactions between an optical pulse and the resonant atoms occur, the quantum mechanical Bloch vector of the atoms undergoes a 2π rotation, and the state of the resonance medium is not varying. It means that the medium is “transparent”. Thus the optical pulse propagates through the medium without loss and distortion. The group velocity of such a coherent pulse depends on the pulse width and is much less than the speed of light due to the SIT effect. Furthermore, the SIT effect is described by the Maxwell-Bloch equations, which have distortionless pulse-train solutions given by the Jacobi elliptic functions [2-4]. Such pulse-train propagation results from the energy of resonant atoms periodically oscillating between the ground state and upper state. In particular, when the Jacobi elliptic modulus is unity, the pulse-train solutions are reduced to single-pulse solutions of hyperbolic secant functions. These single pulse solutions are called SIT solitons. Both SIT solitons and periodic pulse trains have been observed in the experiments [5,6].

More recently, a photonic bandgap (PBG) structure doped with resonant atoms has drawn considerable attention [7-14]. Kozhokin and Kurizki showed that near-resonant gap solitons exist in a Bragg reflector doped with periodic layers of two-level systems [11, 12]. Under the assumption that the resonant absorbers are confined to thin layers, both standing and moving analytic solutions are obtained by using the

slowly varying envelope approximation (SVEA). This specialized PBG model has been extended to study three-dimensional spatiotemporally solitons [13]. In the meantime, Aközbeke and John investigated the fundamental work on SIT solitary waves in PBG materials doped *uniformly* with resonant atoms [14]. For example, they derived single pulse solutions for frequency detuned far from Bragg resonance and frequency detuned near the PBG edge. Notice that a PBG structure has a forbidden band for optical energy, but the SIT provide a mechanism to make it possible that an optical pulse can pass through the PBG medium. Hence such research with respect to SIT propagation through a doped PBG structure is currently a topic of great interest. However, the SIT analytic solution suitably for general frequency detuning and general phase modulation in a uniformly doped PBG medium has never been found. In this paper, we study the SIT in a nonlinear PBG structure doped uniformly with inhomogeneously broadening two-level atoms without using the slowly varying envelope approximation (SVEA). It is shown that the Maxwell-Bloch equations can be reduced to effective nonlinear coupled-mode equations. Analytic distortionless pulse-train solutions to these effective NLCMEs are obtained. It is found that even if the carrier frequency of the pulse train is deeper inside the forbidden band, the pulse trains can propagate through the PBG structure and obey the general SIT phase modulation effect.

The paper is structured as follows: In Section II, the Maxwell-Bloch equations governing the optical pulse propagating in a uniformly doped PBG structure are derived without using the SVEA. We take into account the material dispersion and Kerr nonlinearity of the host medium. In Section III, we solve the Bloch equations and subsequently reduce the Maxwell-Bloch equations to effective nonlinear coupled-mode equations

(NLCMEs). The effective NLCMEs describe that pulse propagation through a uniformly doped PBG structure is equivalent to that through an effective PBG structure without dopants. In Section IV, we solve the effective NLCMEs and obtain exact pulse-train solutions given by the sinusoidal functions. It is also shown that such a pulse train obeys the general SIT phase modulation effect. In Section V, we numerical study the characteristics of the pulse trains in the simplification that the inhomogeneous broadening line shape of the resonant atoms is assumed to be Lorentzian. In Section VI, we compare our studies with the previous research and give the conclusions at last.

II. MAXWELL-BLOCH EQUATIONS WITHOUT USING SVEA

We consider a one-dimensional Bragg grating formed in a host medium with Kerr nonlinearity. The periodic variations of the refractive index inside the grating region is assumed to be [15]

$$\tilde{n}(\omega) = n(\omega) + n_2 |\mathbf{E}|^2 + n_a \cos(2\beta_g z), \quad (2.1)$$

where \mathbf{E} is the electric field in the medium, $n(\omega)$ is the frequency-dependent refractive index, n_2 is the Kerr nonlinear-index coefficient, n_a is the magnitude of the periodic index variations, and β_g is the grating wave number. The two-level atoms with the resonant frequency ω_r and the dipole moment μ are uniformly embedded in this Kerr host medium. From Maxwell's equations, the wave equation describing light propagation in such a medium can be written as

$$\nabla^2 \mathbf{E} - \frac{1}{c^2} \frac{\partial^2 \mathbf{E}}{\partial t^2} - \mu_0 \frac{\partial^2 \mathbf{P}}{\partial t^2} = \mu_0 \frac{\partial^2 \mathbf{P}_R}{\partial t^2}, \quad (2.2)$$

where c is the velocity of light in vacuum, μ_0 is the vacuum permeability, \mathbf{P} is the electric induced polarization including the linear and nonlinear contributions of the host medium, and \mathbf{P}_R is the resonant polarization due to the two-level atoms. In Fourier domain, Eq. (2.2) becomes

$$\nabla^2 \tilde{\mathbf{E}} + \tilde{n}(\omega)^2 \frac{\omega^2}{c^2} \tilde{\mathbf{E}} = -\mu_0 \omega^2 \tilde{\mathbf{P}}_R, \quad (2.3)$$

where $\tilde{\mathbf{E}}$ is the Fourier transform of \mathbf{E} , and $\tilde{\mathbf{P}}_R$ is the Fourier transform of \mathbf{P}_R . The electric field \mathbf{E} propagating along the z direction in such a doped nonlinear PBG structure can be expressed as

$$\mathbf{E}(\mathbf{r}, t) = \frac{1}{2} \hat{x} [E(\mathbf{r}, t) e^{-i\omega_B t} + c.c.]$$

$$= \frac{1}{2} \hat{x} F(x, y) \left\{ [E_+(z, t) e^{i(\beta_g z - \omega_B t)} + E_-(z, t) e^{-i(\beta_g z - \omega_B t)}] + c.c. \right\}, \quad (2.4)$$

where $c.c.$ stands for complex conjugate, \hat{x} is the polarization unit vector of the light assumed to be linearly polarized along the x axis, $F(x, y)$ is the transverse modal distribution, E_+ and E_- are forward and Bragg scattering envelopes, and ω_B is the Bragg frequency. In addition, the macroscopic resonant polarization \mathbf{P}_R caused by the dopants is written as

$$\begin{aligned} \mathbf{P}_R(\mathbf{r}, t) &= \frac{1}{2} \hat{x} [P(\mathbf{r}, t) e^{-i\omega_B t} + c.c.] \\ &= \frac{1}{2} \hat{x} F(x, y) \left\{ [P_+(z, t) e^{i(\beta_g z - \omega_B t)} + P_-(z, t) e^{-i(\beta_g z - \omega_B t)}] + c.c. \right\}, \end{aligned} \quad (2.5)$$

where P_+ and P_- correspond to the polarization envelopes induced by E_+ and E_- , respectively. For simplicity, the quantities of $n_2 |\mathbf{E}|^2$ and n_a are assumed to be much smaller than the refractive index $n(\omega)$ of the host medium, so that they can be treated as perturbations for expanding $\tilde{n}(\omega)^2$ in Eq. (2.3). After substituting Eqs. (2.1), (2.4), and (2.5) into Eq. (2.3), we can convert the resulting equations to time domain by following the perturbation theory of distributed feedback [15] but without using the SVEA. Consequently, the time-domain coupled-mode equations describing pulse propagation in a uniformly doped PBG structure are written as

$$\begin{aligned} \frac{\partial^2 E_{\pm}}{\partial z^2} \pm 2i\beta_0 \frac{\partial E_{\pm}}{\partial z} + 2i\beta_0 \beta_1 \frac{\partial E_{\pm}}{\partial t} - (\beta_1^2 + \beta_0 \beta_2) \frac{\partial^2 E_{\pm}}{\partial t^2} \\ + 2\beta_0 [\Gamma (|E_{\pm}|^2 + 2|E_{\mp}|^2) E_{\pm} + \delta\beta_0 E_{\pm} + \kappa E_{\mp}] \\ + \mu_0 \omega_B^2 (P_{\pm} + \frac{2i}{\omega_B} \frac{\partial P_{\pm}}{\partial t}) = 0, \end{aligned} \quad (2.6)$$

where, β_j ($j=0,1,2$) are determined by the mode-propagation constant $\beta(\omega) = (\omega/c)n(\omega)$ via $\beta_j \equiv d^j \beta / d\omega^j |_{\omega=\omega_B}$, $\delta\beta_0 = \beta_0 - \beta_g$ implies the wave number detuning from the exact Bragg resonance, $\kappa = \pi n_a / \lambda$ is the linear coupling coefficient, $\Gamma = n_2 \omega_B / (cA_{eff})$ is the Kerr nonlinearity coefficient, and the transverse mode function is averaged out by introducing the effective core area

$$A_{eff} = \frac{\left[\int_{-\infty}^{\infty} \int_{-\infty}^{\infty} |F(x, y)|^2 dx dy \right]^2}{\int_{-\infty}^{\infty} \int_{-\infty}^{\infty} |F(x, y)|^4 dx dy}.$$

Note that in arriving at Eqs. (2.6), we expand $\beta(\omega)^2$ in

a Taylor series $\beta(\omega)^2 \approx \beta_0^2 + 2\beta_0\beta_1(\omega - \omega_b) + (\beta_0\beta_2 + \beta_1^2)(\omega - \omega_b)^2$ for converting Eq. (2.3) to time domain beyond the SVEA [16]. Likewise the high-order time derivatives of the polarizations and the coupling terms are neglected.

We now consider the atomic Bloch equations. If the relaxation times of the polarization and population difference are long compared with the pulse width, the relaxation effects of the two-level system can be ignored. Therefore, under the rotating wave approximation, the electric field and the macroscopic polarization satisfy the Bloch equations given by

$$\frac{\partial}{\partial t} P = -i\Delta\omega P + i\frac{\mu}{\hbar} WE, \quad (2.7a)$$

$$\frac{\partial}{\partial t} W = -i\frac{\mu}{2\hbar}(EP^* - E^*P), \quad (2.7b)$$

where $\Delta\omega$ is defined by $\Delta\omega = \omega_r - \omega_b$, $W = \mu(N_1 - N_2)$ is the macroscopic population difference multiplied by μ between the ground state (N_1) and upper state (N_2) of the two-level system. The complex envelopes E_{\pm} and P_{\pm} can be further written as

$$E_{\pm}(z, t) = a_{\pm}(z, t) \exp[i\varphi_{\pm}(z, t)], \quad (2.8a)$$

$$P_{\pm}(z, t) = [U_{\pm}(z, t) + iV_{\pm}(z, t)] \exp[i\varphi_{\pm}(z, t)], \quad (2.8b)$$

where $a_{\pm}(z, t)$ are real envelopes, $\varphi_{\pm}(z, t)$ are phase functions, $U_{\pm}(z, t)$ correspond to the dispersion (in phase) induced by the resonant atoms, and $V_{\pm}(z, t)$ correspond to the absorption (in quadrature) caused by the resonant atoms. Moreover, the Bloch vectors (u_{\pm}, v_{\pm}, w) relate the macroscopic polarization and population difference as follows:

$$(U_{\pm}, V_{\pm}, W) = \int_{-\infty}^{\infty} (u_{\pm}, v_{\pm}, w) g(\Delta\omega) d(\Delta\omega), \quad (2.9)$$

where $u_{\pm}(\Delta\omega, z, t)$, $v_{\pm}(\Delta\omega, z, t)$, and $w(\Delta\omega, z, t)$ are the components of polarization and population difference contributed from the atoms with frequency $\Delta\omega$ detuned from ω_b , and $g(\Delta\omega)$ is the normalized inhomogeneous-broadening line-shape function. To keep a closed set of Bloch equations, we assume that

$$\varphi_{\pm}(z, t) = \phi(z, t) \pm \psi(z, t), \quad (2.10a)$$

$$w = w_0 + 2w_1 \cos[2\psi(z, t) + 2\beta_g z]. \quad (2.10b)$$

After substituting Eqs. (2.4), (2.5) and Eqs. (2.8)-(2.10)

into Eqs. (2.7), the Bloch equations are expressed as

$$\frac{\partial u_{\pm}}{\partial t} = (\Delta\omega + \frac{\partial\varphi_{\pm}}{\partial t})v_{\pm}, \quad (2.11a)$$

$$\frac{\partial v_{\pm}}{\partial t} = -(\Delta\omega + \frac{\partial\varphi_{\pm}}{\partial t})u_{\pm} + \frac{\mu}{\hbar}(a_{\pm}w_0 + a_{\mp}w_1), \quad (2.11b)$$

$$\frac{\partial w_0}{\partial t} = -\frac{\mu}{\hbar}(a_{+}v_{+} + a_{-}v_{-}), \quad (2.11c)$$

$$\frac{\partial w_1}{\partial t} = -\frac{\mu}{2\hbar}(a_{+}v_{-} + a_{-}v_{+}). \quad (2.11d)$$

In Eqs. (2.11), we have neglected terms oscillating as $\exp(\pm i3\beta_g z)$.

III. EFFECTIVE NLCMES FOR THE MAXWELL-BLOCH EQUATIONS

In this section, we reduce the Maxwell-Bloch equations to effective NLCMEs for coherence light propagating in a nonlinear PBG structure doped uniformly with inhomogeneously broadening two-level atoms. In order to obtain the analytic solution we assume $v_{\pm}(\Delta\omega, z, t)$ are in factorized forms [4, 14, 17]

$$v_{\pm}(\Delta\omega, z, t) = v_{\pm}(0, z, t) f(\Delta\omega), \quad (3.1)$$

where $f(\Delta\omega)$ is known as the dipole spectra-response function and is normalized as $f(0) = 1$. Integrating Eqs. (2.11a), we have

$$u_{\pm}(\Delta\omega, z, t) = [u_1^{\pm}(z, t) + u_2^{\pm}(z, t)\Delta\omega] f(\Delta\omega), \quad (3.2)$$

where u_1^{\pm} and u_2^{\pm} are defined as

$$\frac{\partial u_1^{\pm}}{\partial t} \equiv v_1^{\pm} \frac{\partial\varphi_{\pm}}{\partial t}, \quad (3.3a)$$

$$\frac{\partial u_2^{\pm}}{\partial t} \equiv v_2^{\pm}, \quad (3.3b)$$

Similarly, by integrating Eq. (2.11c) and (2.11d), we obtain

$$w_0(\Delta\omega, z, t) = w_i - [w_0^+(z, t) + w_0^-(z, t)] f(\Delta\omega), \quad (3.4a)$$

$$w_1(\Delta\omega, z, t) = -\frac{1}{2} [w_1^+(z, t) + w_1^-(z, t)] f(\Delta\omega). \quad (3.4b)$$

In Eqs. (3.4), w_i is the initial population difference and it is assumed in the ground state of the two-level system,

i.e., $w_i = N_D \mu$, where $N_D = N_1 + N_2$ is the doping concentration of the resonant atoms. Likewise w_0^\pm and w_1^\pm are defined as

$$\frac{\partial w_0^+}{\partial t} \equiv \frac{\mu}{\hbar} a_+ v_1^+ \quad \text{and} \quad \frac{\partial w_0^-}{\partial t} \equiv \frac{\mu}{\hbar} a_- v_1^-, \quad (3.5a)$$

$$\frac{\partial w_1^+}{\partial t} \equiv \frac{\mu}{\hbar} a_+ v_1^- \quad \text{and} \quad \frac{\partial w_1^-}{\partial t} \equiv \frac{\mu}{\hbar} a_- v_1^+. \quad (3.5b)$$

Substituting Eqs. (3.1)-(3.5) into Eqs. (2.11b), we have

$$\begin{aligned} \frac{\partial w_i^\pm}{\partial t} = & -\frac{\partial \varphi_\pm}{\partial t} u_i^\pm - \frac{\mu}{\hbar} (w_0^+ + w_0^-) a_\pm + \\ & \left[-\frac{\mu(w_1^+ + w_1^-)}{2\hbar} a_\mp - (u_i^\pm + \frac{\partial \varphi_\pm}{\partial t} u_2^\pm) \Delta \omega - u_2^\pm \Delta \omega^2 + \frac{\mu w_i}{\hbar} \frac{a_\pm}{f(\Delta \omega)} \right] \end{aligned} \quad (3.6)$$

The terms in square brackets in Eqs. (3.6) should be independent of $\Delta \omega$. Therefore, we have

$$f(\Delta \omega) = (1 + c_1 \Delta \omega + c_2 \Delta \omega^2)^{-1}, \quad (3.7)$$

and

$$u_1^\pm = -\frac{\partial \varphi_\pm}{\partial t} u_2^\pm + c_1 \frac{\mu}{\hbar} a_\pm w_{0i}, \quad (3.8a)$$

$$u_2^\pm = c_2 \frac{\mu}{\hbar} a_\pm w_{0i}, \quad (3.8b)$$

where c_1 and c_2 are the constants to be determined. Substituting Eqs. (3.3b) and (3.8) into Eqs. (3.1), (3.2), (3.4), and (3.5), we obtain

$$u_\pm = [c_1 - (\frac{\partial \varphi_\pm}{\partial t} - \Delta \omega) c_2] \frac{\mu}{\hbar} w_i f(\Delta \omega) a_\pm(z, t), \quad (3.9a)$$

$$v_\pm = c_2 \frac{\mu}{\hbar} w_i f(\Delta \omega) \frac{\partial}{\partial t} a_\pm(z, t), \quad (3.9b)$$

$$w_0 = w_i - \frac{c_2}{2} \left(\frac{\mu}{\hbar}\right)^2 w_i f(\Delta \omega) [a_+^2(z, t) + a_-^2(z, t)], \quad (3.9c)$$

$$w_1 = -\frac{c_2}{2} \left(\frac{\mu}{\hbar}\right)^2 w_i f(\Delta \omega) [a_+(z, t) a_-(z, t)]. \quad (3.9d)$$

Then substituting Eqs. (3.9) into Eqs. (2.11a) and (2.11b), we have

$$2 \frac{\partial a_\pm}{\partial t} \frac{\partial \varphi_\pm}{\partial t} + \frac{\partial^2 \varphi_\pm}{\partial t^2} a_\pm = \frac{c_1}{c_2} \frac{\partial a_\pm}{\partial t}, \quad (3.10a)$$

$$\frac{\partial^2 a_\pm}{\partial t^2} = \left[\frac{1}{c_2} - \frac{c_1}{c_2} \left(\frac{\partial \varphi_\pm}{\partial t}\right) + \left(\frac{\partial \varphi_\pm}{\partial t}\right)^2 \right] a_\pm - \frac{\mu^2}{2\hbar^2} (a_\pm^2 + 2a_\mp^2) a_\pm. \quad (3.10b)$$

Eqs. (3.10) are the keys to this paper. These key results not only describe the coupling nature between the envelopes and phases of the forward and Bragg scattering fields in the PBG structure, but also lead to the general SIT chirping equation, which will be studied in the next section. Now we show that using Eqs. (3.10) can reduce the Maxwell-Bloch equations to effective NLMEs. Using Eqs. (2.7)-(2.8), (3.9), and (3.10) to reduce $\partial^2 E_\pm / \partial t^2$ and $\mu_o \omega_o^2 [P_\pm + (2i/\omega_o)(\partial P_\pm / \partial t)]$, we obtain

$$\begin{aligned} \frac{\partial^2 E_\pm}{\partial t^2} = & i \frac{c_1}{c_2} \frac{\partial E_\pm}{\partial t} + \frac{1}{c_2} E_\pm \\ & - \frac{1}{2} \left(\frac{\mu}{\hbar}\right)^2 (|E_\pm|^2 + 2|E_\mp|^2) E_\pm, \end{aligned} \quad (3.11a)$$

$$\begin{aligned} \mu_o \omega_o^2 (P_\pm + \frac{2i}{\omega_o} \frac{\partial P_\pm}{\partial t}) = & s \left[(c_1 - \frac{2}{\omega_o}) I_1 + c_2 I_2 \right] E_\pm \\ & + i s c_2 (I_1 + \frac{2}{\omega_o} I_2) \frac{\partial E_\pm}{\partial t} \\ & + s \frac{c_2}{\omega_o} I_1 \left(\frac{\mu}{\hbar}\right)^2 (|E_\pm|^2 + 2|E_\mp|^2) E_\pm, \end{aligned} \quad (3.11b)$$

where s is $s = \mu_o \omega_o^2 (\mu/\hbar) w_i$, and two integral constants I_1 and I_2 are defined by

$$I_1 = \int_{-\infty}^{\infty} f(\Delta \omega) g(\Delta \omega) d(\Delta \omega), \quad (3.12a)$$

$$I_2 = \int_{-\infty}^{\infty} \Delta \omega f(\Delta \omega) g(\Delta \omega) d(\Delta \omega). \quad (3.12b)$$

Substituting Eqs. (3.11) into Eqs. (2.6), we obtain

$$\begin{aligned} \frac{\partial^2 E_\pm}{\partial z^2} \pm 2i\beta_o \frac{\partial E_\pm}{\partial z} + 2i\beta_o \beta_i^e \frac{\partial E_\pm}{\partial t} \\ + 2\beta_o [\delta\beta_e E_\pm + \kappa E_\mp + \Gamma_e (|E_\pm|^2 + 2|E_\mp|^2) E_\pm] = 0, \end{aligned} \quad (3.13)$$

where the effective parameters are

$$\beta_i^e = \beta_i - (\beta_i^2 + \beta_o \beta_2) \frac{c_1}{2\beta_o c_2} + \frac{s c_2}{2\beta_o} (I_1 + \frac{2}{\omega_o} I_2), \quad (3.14a)$$

$$\Gamma_e = \Gamma + (\beta_1^2 + \beta_o \beta_2) \frac{\mu^2}{4\beta_o \hbar^2} + \frac{s c_2}{2\beta_o \omega_o} I_1 \frac{\mu^2}{\hbar^2}, \quad (3.14b)$$

$$\delta\beta_e = \delta\beta_o + \frac{s}{2\beta_o} \left[(c_1 - \frac{2}{\omega_o}) I_1 + c_2 I_2 - \frac{\beta_1^2 + \beta_o \beta_2}{s c_2} \right]. \quad (3.14c)$$

Consequently, we have reduced Eqs. (2.6) to

effective NLCMEs beyond the SVEA. The effective NLCMEs describe that pulse propagation through a uniformly doped PBG structure is equivalent to that through an effective PBG structure without dopants. These effective NLCMEs are referred to as the Bloch-NLCMEs. It is notice that the analytic solutions describing pulse propagation in a doped nonlinear PBG structure have to satisfy both Eqs. (3.10) and Eqs. (3.13).

VI. EXACT ANALYTIC SOLUTIONS TO THE BLOCH-NLCMES

Now we start solving the Bloch-NLCMEs to obtain analytic solutions. By making the moving coordinate transformation $\tau = t - z/v_g$ and $\xi = z$, the Bloch-NLCMEs are rewritten to the forms:

$$\begin{aligned} & \frac{\partial^2 E_{\pm}}{\partial \xi^2} - \frac{2}{v_g} \frac{\partial^2 E_{\pm}}{\partial \tau \partial \xi} \pm 2i\beta_o \frac{\partial E_{\pm}}{\partial \xi} + 2i\beta_o (\beta_1^e \mp \frac{1}{v_g}) \frac{\partial E_{\pm}}{\partial \tau} + \frac{1}{v_g^2} \frac{\partial^2 E_{\pm}}{\partial \tau^2} \\ & + 2\beta_o \delta\beta_e E_{\pm} + 2\beta_o [\Gamma_e (|E_{\pm}|^2 + 2|E_{\mp}|^2) E_{\pm} + \kappa E_{\mp}] = 0. \end{aligned} \quad (4.1)$$

To solve the Bloch-NLCMEs, we seek the solutions of the forms

$$E_{\pm}(z, t) = a_{\pm}(\tau) \exp[i\varphi_{\pm}(\tau) + i\Delta\beta_o \xi]. \quad (4.2)$$

Eqs. (4.2) indicate that the phase functions are $\phi(z, t) = \phi(\tau) + \Delta\beta_o \xi$ and $\psi(z, t) = \psi(\tau)$, where $\Delta\beta_o$ represents the change of the propagation constant due to the resonant atoms and Kerr nonlinearity. Substituting Eq. (3.11a) and (4.2) into Eqs. (4.1), and using the new variables of optical field $E_{\pm}(\tau) = a_{\pm}(\tau) \exp[i\varphi_{\pm}(\tau)]$ to express Eqs. (4.1), we have

$$+i(\bar{\beta}_1 \mp \frac{1}{v_g}) \frac{\partial E_{\pm}}{\partial \tau} + (\delta\bar{\beta}_o \mp \Delta\beta_o) E_{\pm} + \bar{\Gamma} (|E_{\pm}|^2 + 2|E_{\mp}|^2) E_{\pm} + \kappa E_{\mp} = 0, \quad (4.3)$$

where $\bar{\Gamma} = \Gamma_e - \mu^2 / (4\beta_o v_g^2 \hbar^2)$, $\bar{\beta}_1 = \beta_1^e + c_1 / (2\beta_o c_2 v_g^2) - \Delta\beta_o / (v_g \beta_o)$, and $\delta\bar{\beta}_o = \delta\beta_e + 1 / (2\beta_o c_2 v_g^2) - \Delta\beta_o^2 / 2\beta_o$. The forms of Eqs. (4.3) are equivalent to the general NLCMEs that have moving gap-soliton solutions describing distortionless pulse propagation through undoped PBG structure [18]. However, we will show in the following that such gap soliton solutions cannot satisfy Eqs. (3.10). Separating the real parts and imaginary parts of Eqs. (4.3), we obtain the following differential equations:

$$(\bar{\beta}_1 \mp \frac{1}{v_g}) \frac{\partial a_{\pm}}{\partial \tau} \mp \kappa a_{\mp} \sin(2\psi) = 0, \quad (4.4a)$$

$$\begin{aligned} & -(\bar{\beta}_1 \mp \frac{1}{v_g}) \frac{\partial \varphi_{\pm}}{\partial \tau} a_{\pm} + (\delta\bar{\beta}_o \mp \Delta\beta_o) a_{\pm} \\ & + \bar{\Gamma} a_{\pm}^3 + 2\bar{\Gamma} a_{\mp}^2 a_{\pm} + \kappa a_{\mp} \cos(2\psi) = 0, \end{aligned} \quad (4.4b)$$

Eqs. (4.4) possess two first integrals [19]

$$\beta_{1n} a_+^2 + \beta_{1p} a_-^2 = c_0, \quad (4.5a)$$

$$\begin{aligned} \beta_{1p} \beta_{1n} \cos(2\psi) a_+ a_- &= \frac{\beta_{1n}}{\kappa} (\Delta\beta_o \bar{\beta}_1 - \frac{\delta\bar{\beta}_o}{v_g}) a_+^2 \\ &+ \frac{\bar{\Gamma}}{4\kappa} \beta_{1n} \beta_{3n} a_+^4 + \frac{\bar{\Gamma}}{4\kappa} \beta_{1p} \beta_{3p} a_-^4 + c_3, \end{aligned} \quad (4.5b)$$

where c_0 and c_3 are integration constants, and $\beta_{1p} = \bar{\beta}_1 + 1/v_g$, $\beta_{1n} = \bar{\beta}_1 - 1/v_g$, $\beta_{3p} = \bar{\beta}_1 + 3/v_g$ and $\beta_{3n} = \bar{\beta}_1 - 3/v_g$. Substituting Eqs. (4.4a) and Eq. (4.5a) into Eq. (4.5b), we have a differential equation for a_{\pm}^2 :

$$\begin{aligned} & (c_0 \beta_{1p} \beta_{1n}^2 a_+^2 - \beta_{1p} \beta_{1n}^3 a_+^4) - \frac{\beta_{1p}^2 \beta_{1n}^4}{4\kappa^2} \left[\frac{\partial (a_+^2)}{\partial \tau} \right]^2 \\ &= \left[(c_3 + c_0^2 \frac{\bar{\Gamma}}{4\kappa} \frac{\beta_{3p}}{\beta_{1p}}) + \frac{\bar{\Gamma}}{4\kappa} \beta_{1n} (\beta_{3n} + \frac{\beta_{3p}}{\beta_{1p}} \beta_{1n}) a_+^4 \right. \\ & \left. + \frac{\beta_{1n}}{\kappa} (\Delta\beta_o \bar{\beta}_1 - \frac{\delta\bar{\beta}_o}{v_g}) - \frac{1}{2} c_0 \bar{\Gamma} \frac{\beta_{3p}}{\beta_{1p}} \right] a_+^2. \end{aligned} \quad (4.6)$$

By defining $S = a_{\pm}^2$, Eq. (4.6) can be expressed as

$$\frac{(\dot{S})^2}{4} + \gamma_0 + \gamma_1 S + \gamma_2 S^2 + \gamma_3 S^3 + \gamma_4 S^4 = 0, \quad (4.7)$$

where the expressions of γ_m ($m=0, 1, 2, 3, 4$) for Eq. (4.7) will be discussed later. Eq. (4.7) can describe the motion of a solitary wave by analogy with that of a classical particle moving in a potential. Therefore, analytic solutions to Eq. (4.7) have been extensively studied for grating solitons and SIT theory. The well-known solutions include single-pulse solitary waves (for $\gamma_0 = \gamma_1 = 0$) [18,19], single-pulse solitons (for $\gamma_0 = \gamma_1 = \gamma_4 = 0$) and Jacobi elliptic soliton-trains (for $\gamma_4 = 0$) [2,4,14]. From a mechanical analogy viewpoint, a single-pulse solution corresponds to a particle resting at a position of zero displacement, and a pulse-train solution corresponds to a particle oscillating between two positions. Notice that all the above solutions are obtained under $\gamma_2 \neq 0$ and $\gamma_3 \neq 0$. However, for a uniformly doped nonlinear PBG structure, the Bloch-NLCMEs constrain the quantities of γ_3 . Indeed, we subsequently show that γ_3 has to be zero for exact

solutions to Eq. (4.6). Using $\partial/\partial t = \partial/\partial \tau$ and integrating Eq. (3.10a), we obtain

$$\frac{\partial \varphi_{\pm}}{\partial \tau} = -\Omega + \frac{c_4^{\pm}}{a_{\pm}^2}, \quad (4.8)$$

where $\Omega = -c_1/(2c_2)$ and c_4^{\pm} are integration constants. Eqs. (4.8) describe the general phase modulation, or pulse chirping in the SIT. The constant Ω indicates that the carrier frequency of the optical field is shifted to $\omega_b + \Omega$ by the SIT effect. Likewise the shifted instantaneous frequency is inversely proportional to the pulse intensity. The general chirping relation has been studied for the SIT in a resonance medium without PBG structure [4]. Substituting Eqs. (4.8) and Eq. (4.5a) into Eq. (3.10b), and then integrating the resulting equation, we obtain

$$\begin{aligned} \frac{(\dot{S})^2}{4} + (c_4^+)^2 - c_3 S + \left(\Omega^2 + \frac{\mu^2 c_0}{\hbar^2 \beta_{1p}} - \frac{1}{c_2} \right) S^2 \\ + \frac{1}{2} \left(\frac{\mu}{\hbar} \right)^2 \left(\frac{1}{2} - \frac{\beta_m}{\beta_{1p}} \right) S^3 = 0, \end{aligned} \quad (4.9)$$

where c_5 is another integration constant. Comparing Eq. (4.6), Eq. (4.7) and Eq. (4.9), we undergo the constraint $\gamma_3 = 0$ resulting from $\gamma_4 = 0$. These constraints lead to $\bar{\beta}_1 = 3/v_g$ and $\bar{\Gamma} = 0$. Hence γ_0 , γ_1 and γ_2 are determined as

$$\gamma_0 = \frac{1}{256} \kappa^2 c_3^2 v_g^6 = (c_4^+)^2, \quad (4.10a)$$

$$\gamma_1 = \frac{1}{64} \kappa c_3 (3\Delta\beta_0 - \delta\bar{\beta}_0) v_g^4 - \frac{1}{16} c_0 \kappa^2 v_g^3 = -c_5, \quad (4.10b)$$

$$\begin{aligned} \gamma_2 = \frac{1}{64} (3\Delta\beta_0 - \delta\bar{\beta}_0)^2 v_g^2 + \frac{1}{8} \kappa^2 v_g^2 \\ = \Omega^2 + \frac{\mu^2}{4\hbar^2} c_0 v_g - \frac{1}{c_2}. \end{aligned} \quad (4.10c)$$

Since γ_3 has to be zero, the exact single-pulse and Jacobi pulse-train solutions cannot exist for the Bloch-NLCMEs equations. Nevertheless, Eq. (4.9) can be integrated to yield

$$\int_{a_+(0)}^{a_+} \frac{a_+ da_+}{\sqrt{-a_+^4 - (\gamma_1 a_+^2 + \gamma_0)/\gamma_2}} \equiv \int_{a_+(0)}^{a_+} \frac{a_+ da_+}{\sqrt{P_4(a_+)}} = \sqrt{\gamma_2} \tau. \quad (4.11)$$

Because $\gamma_0 > 0$ and $\gamma_2 > 0$ from Eqs. (4.10), we have to restrict $\gamma_1 < 0$ ($c_5 > 0$) for $P_4(a_+) > 0$. The solution to Eq. (4.11) depends on the roots of

$P_4(a_+)$. Thus we assume $P_4(a_+) = (a_p^2 - a_+^2) \times (a_+^2 - a_q^2)$, where $0 \leq a_q \leq a_+(\tau) \leq a_p$. Then Eq. (4.11) have an exact analytic solution written by

$$a_+ = \sqrt{a_p^2 - (a_p^2 - a_q^2) \sin^2(\sqrt{\gamma_2} \tau)}, \quad (4.12a)$$

where $a_p^2 = c_5/2\gamma_2 + \sqrt{(c_5/2\gamma_2)^2 - \gamma_0/\gamma_2}$ and $a_q^2 = c_5/2\gamma_2 - \sqrt{(c_5/2\gamma_2)^2 - \gamma_0/\gamma_2}$. From Eq. (4.5a) and Eqs. (4.8), $a_-(\tau)$, $\varphi_+(\tau)$ and $\varphi_-(\tau)$ are obtained as follow:

$$a_- = \frac{1}{\sqrt{2}} \sqrt{\left(\frac{1}{2} c_0 v_g - a_p^2 \right) + (a_p^2 - a_q^2) \sin^2(\sqrt{\gamma_2} \tau)}, \quad (4.12b)$$

$$\varphi_+ = -\Omega \tau + \frac{c_4^+}{a_p a_q \sqrt{\gamma_2}} \tan^{-1} \left[\frac{a_q}{a_p} \tan(\sqrt{\gamma_2} \tau) \right] + \Psi_+, \quad (4.12c)$$

$$\begin{aligned} \varphi_- = -\Omega \tau + \frac{4c_4^-}{\sqrt{\gamma_2 (c_0 v_g - 2a_p^2)(c_0 v_g - 2a_q^2)}} \\ \times \tan^{-1} \left[\sqrt{\frac{c_0 v_g - 2a_q^2}{c_0 v_g - 2a_p^2}} \tan(\sqrt{\gamma_2} \tau) \right] + \Psi_-, \end{aligned} \quad (4.12d)$$

where Ψ_+ and Ψ_- are integration constant. As a result, we have obtained exact analytic solutions to the Bloch-NLCMEs. Physically, these solutions demonstrate that both the forward and Bragg scattering fields are infinite CW electromagnetic waves whose amplitudes are modulated periodically with a period $T_p = \pi/\sqrt{\gamma_2}$. These periodic pulse trains propagate distortionlessly in the same direction. Thus the group velocity of the Bragg scattering field is in the direction opposite to its phase velocity. Such distortionless propagation results from the two-level atoms periodically absorbing energy from one part of the wave and then returning the energy to an adjacent part [3]. Likewise these coherent photon-atom interactions balance with the grating dispersion and Kerr nonlinearity. Therefore, SIT occurs and the optical field overcomes the forbidden band and passes through the PBG structure.

V. NUMERICAL STUDY OF THE PULSE-TRAIN CHARACTERISTICS

To study the distortionless pulse trains, we have to further derive all undetermined constants. For the following discussions, we restrict our attention to the optical field without carrier frequency shift, i. e., $\Omega = 0$. In addition, the inhomogeneous broadening line shape of the resonant atoms is assumed to be Lorentzian and written as

$$g(\Delta\omega) = \frac{\Delta\omega_a}{2\pi} \frac{1}{\Delta\omega^2 + (\Delta\omega_a/2)^2}, \quad (5.1)$$

where $\Delta\omega_a = 2\pi f_a$ is the full width at half maximum (FWHM) of $g(\Delta\omega)$. Substituting Eq. (5.1) and Eq.(3.7) into the definitions of I_1 and I_2 in Eqs. (3.12), we find that $I_1 = 2/(\sqrt{c_2}\Delta\omega_a)$ and $I_2 = 0$ for $\Delta\omega_a \gg 1/\sqrt{c_2}$ [16] which will be justified later. From $\bar{\Gamma} = 0$, $\bar{\beta}_1 = 3/v_g$ and Eqs. (3.14), both c_2 and $\Delta\beta_0$ are first obtained as a function of the group velocity v_g :

$$c_2 = \frac{\Delta\omega_a^2 \omega_0^2}{16s^2 \mu^4 v_g^4} [4\hbar^2 v_g^2 \beta_0 \Gamma - \mu^2 + v_g^2 \mu^2 (\beta_1^2 + \beta_0 \beta_2)]^2, \quad (5.2a)$$

$$\Delta\beta_0 = \frac{1}{4} v_g [\beta_1^2 \omega_0 + \beta_0 (4\beta_1 + \beta_2 \omega_0 + \frac{4\hbar^2 \Gamma \omega_0}{\mu^2})] - \frac{\omega_0}{4v_g} - 3\beta_0. \quad (5.2b)$$

Substituting Eqs. (4.12) and $\bar{\Gamma} = 0$ into Eqs. (4.4b), and then comparing the expressions of $\cos(2\psi)$ derived from the upper- and lower- sign equation of Eqs. (4.4b), we have

$$\delta\bar{\beta}_0 = \frac{\Delta\beta_0}{3} = \left(\frac{1}{2\beta_0 c_2}\right) \frac{1}{v_g^2} + \delta\beta_c - \frac{\Delta\beta_0^2}{2\beta_0}, \quad (5.3a)$$

$$c_4^- = \frac{1}{12} c_0 \Delta\beta_0 v_g^2 + \frac{c_4^+}{2}. \quad (5.3b)$$

By substituting Eq. (5.2b) into Eq. (5.3a), not only $\delta\bar{\beta}_0$ is expressed as functions of the group velocity v_g , but also the group velocity is determined for given parameters of the medium. Consequently, the pulse-train period $T_p = \pi/\sqrt{\gamma_2}$ and the integration constant c_0 are further obtained from Eq. (4.10c). On the other hand, in order to obtain the integration constants c_3 , c_4^\pm , and c_5 , we define the total intensity of the forward and Bragg scattering field as follows [20]:

$$I_T \equiv a_+(\tau)^2 + a_-(\tau)^2 = I_0 + I_m \cos^2(\sqrt{\gamma_2}\tau), \quad (5.4)$$

where $I_0 = c_0 v_g / 4 + a_q^2 / 2$ is the background intensity and $I_m = (a_p^2 - a_q^2) / 2$ is the modulated intensity of the total field. The relationship between the optical power and optical intensity is $P_T = (n_0 / 2)(\sqrt{\epsilon_0 / \mu_0}) A_{\text{eff}} I_T$, where ϵ_0 is the vacuum permittivity, n_0 is the

refractive index at the Bragg wavelength of the host medium. In this paper, we are interested in the contrast between the total field and its modulated amplitude. Thus we define the contrast $\eta = I_m / (I_0 + I_m)$. Then the integration constants c_3 , c_4^\pm , and c_5 can be determined for a given η by using the expressions of I_0 , I_m , a_p and a_q in conjunction with Eqs. (4.10). Moreover, for the constant phase parameters Ψ_+ and Ψ_- , we can assume $\Psi_+ = \Psi_- = 0$ for chirped envelopes ($c_4^\pm \neq 0$). However, for an unchirped pulse train, the forward and Bragg scattering field have to satisfy a constant phase difference $\Psi_+ - \Psi_- = l\pi/4$ (l : odd number) obtained from Eqs. (4.4a). Such an unchirped case leads to $\Delta\beta_0 = 0$ and $c_3 = 0$ from Eqs. (4.4b) and Eqs. (4.10a), respectively. Therefore, a_\pm are reduced to

$$a_+(\tau) = a_p \left| \cos(\sqrt{\gamma_2}\tau) \right|, \quad (5.5a)$$

$$a_-(\tau) = a_p \left| \sin(\sqrt{\gamma_2}\tau) \right| / \sqrt{2}. \quad (5.5b)$$

These results lead to $I_0 = c_0 v_g / 4 = a_p^2 / 2$ that cannot be zero for the existence of the pulse train. Consequently, there must be a dc term in the total intensity of the pulse train.

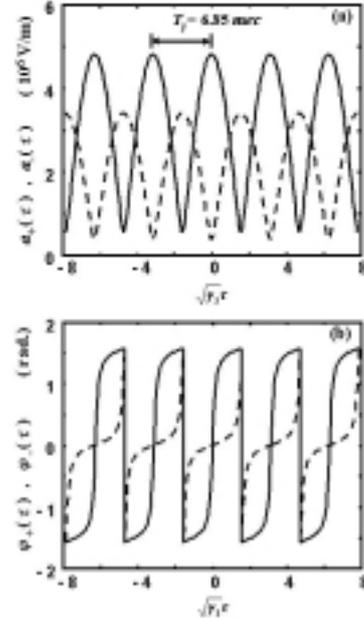


FIG. 1. (a) Envelopes and (b) phases of the optical forward field (solid curves) and Bragg scattering field (dashed curves) as functions of a scaled time $\sqrt{\gamma_2}\tau$. The pulse-train period is $T_p = \pi/\sqrt{\gamma_2} = 6.85 \text{ nsec}$; and the group velocity is $v_g = 1.29 \times 10^6 \text{ m/sec}$ resulting in a appropriate $\Delta\beta_0 = -0.00169 \text{ m}^{-1}$ and corresponding to 1/250 of the speed of light in the bare Kerr-host medium.

In order to illustrate the pulse trains, we use the following material parameters: The Kerr host medium is silica-based material with $n_0=1.45$, $A_{\text{eff}}=50\mu\text{m}^2$, $\beta_0=5.9\times 10^6\text{m}^{-1}$, $\beta_1=4.8\times 10^9\text{sec/m}$, $\beta_2=-20\text{psec}^2/\text{km}$ and $\Gamma=4.86\times 10^{-16}\text{m/V}^2$ ($n_2=1.2\times 10^{-22}\text{m}^2/\text{V}^2$) at 1550nm wavelength region. The coupling coefficient of the Bragg grating is $\kappa=10\text{cm}^{-1}$ corresponding to the index vibration $n_a=0.006$ at the Bragg wavelength $\lambda_B=1553\text{nm}$. Here we focus the frequency on the exact Bragg resonance, i.e., $\delta\beta_0=0\text{cm}^{-1}$. For the two-level atoms, we assume that $\mu=1.4\times 10^{-32}\text{C}\cdot\text{m}$, $\Delta f_a=1472\text{GHz}$ and $N_D=8.0\times 10^{24}\text{m}^{-3}$ corresponding to the typical 1000ppm doping concentration of erbium atoms. By using the above parameters, Fig.1 shows the envelopes and phases of the optical forward field (solid curves) and Bragg scattering field (dashed curves) as functions of a scaled time $\sqrt{\gamma_2}\tau$. Note that the resulting group velocity is $v_g=1.29\times 10^6\text{m/sec}$ being consistent with the assumption of $\Delta\omega_a \gg 1/\sqrt{c_2}$. The group velocity of this forward propagating energy is substantially less than the speed of light in the bare Kerr-host medium because both SIT and Bragg scattering slow down the light. Fig. 2 shows the total power of such slow light as a function of $\sqrt{\gamma_2}\tau$. The peak power is $P_0+P_M=2.24\text{W}$ and occurs when $\varphi_+(\tau)=\varphi_-(\tau)=0$. Furthermore, the components of the Bloch vectors (u_{\pm}, v_{\pm}, w) are obtained by substituting Eq. (4.12) into Eqs. (3.9). Fig. 3 shows the normalized population difference as a function of $\sqrt{\gamma_2}\tau$ and $\beta_g\xi$. Clearly, the magnitude of the population difference is modulated periodically with the period T_p , and the time average of the population difference varies periodically along the propagating distance. Such energy exchanges between the upper state and the lower state lead to the distortionless pulse trains, even if the central frequency of the optical envelopes is deeper inside the forbidden band. Finally, we emphasize that the pulse-train period $T_p=6.85\text{nsec}$ corresponds to each pulse width (FWHM) $T_w=0.5T_p=3.425\text{nsec}$. Recalling that for deriving Eqs. (2.11), we assume the relaxation times of the resonant atoms are long compared with the pulse width T_w . However, at 4.2K , the relaxation times of erbium atoms are $T_1=10\text{msec} (\gg T_w)$ for the population difference, and $T_2=10\text{nsec} (> T_w)$ for the polarizations. Accordingly, the pulse width, strictly speaking, is not consistent with $T_2 \gg T_w$. From an experimental viewpoint, the medium would incoherently absorb the pulse energy because the total pulse-train length should be much less than T_1 and T_2 . Nevertheless, it will be interesting to find out the suitable materials and

conditions to experimentally study the distortionless propagation.

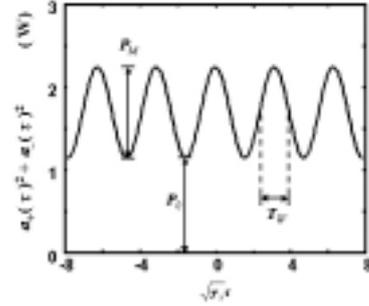


FIG. 2. Total power of the pulse train as a function of a scaled times $\sqrt{\gamma_2}\tau$. For $c_5 > 0$, the contrast η has to satisfy $\eta < 0.5$. Hence we choice $\eta = 0.49$ so that the background optical power is $P_0=1.10\text{W}$ and the amplitude of the modulated power is $P_M=1.14\text{W}$. Each pulse width is $T_w=0.5T_p=3.425\text{nsec}$ (FWHM).

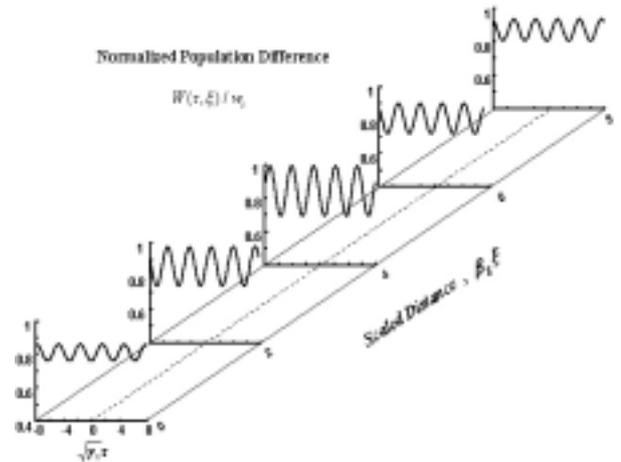


FIG. 3. Normalized population difference as a function of a scaled time $\sqrt{\gamma_2}\tau$ and a scaled distance $\beta_g\xi$. Clearly, the magnitude of the population difference is modulated periodically with the same period $T_p=6.85\text{nsec}$; likewise the time average of the population difference varies periodically along the propagating distance.

VI. DISCUSSIONS AND CONCLUSIONS

For the research of optical pulses propagating through a doped Bragg reflector, Mantsyzov first studied pulse propagation in a discrete one-dimensional medium made of two-level atoms [21]. Subsequently, Kozhekin and Kurizki extended this discrete model to continuous medium in which thin layers of two-level atoms are periodically placed at a one-dimensional PBG structure [11-13]. These studies all assume that the resonant absorbers are confined to *thin layers*. Aközbe and John first studied the SIT solitary waves in a

uniformly doped nonlinear PBG material [14]. In this present paper, we adopt the similar uniformly doped PBG model to study SIT pulse-train propagation. However, in contrast with Ref. [14], our model is more general than that in Ref. [14]: (i) In our uniformly doped PBG model, we derive the Maxwell-Bloch equation without using the slowly varying envelope approximation. The formation of the SIT effects require ultrashort pulses with their pulse widths being shorter than the relaxation times of the resonant atoms, but the SVEA is not valid for a ultrashort pulse. Thus we use the model without making the SVEA. Moreover, in Ref. [14], the authors emphasize that they have neglected the linear contribution to the dispersion relation arising from the two-level atoms. Hence the allowed concentration of dopant atoms are limited for their SVEA model. In Ref. [17], it has been found that SIT could induce an additional negative dispersion of which it has not been predicted by the SIT theory under SVEA. Since the Maxwell-Bloch equation without using the SVEA can reduce to Bloch-NLCMEs, these effective NLCMEs completely involve the SIT-induced negative dispersion and the effective grating dispersion. (ii) The phase functions of the forward and Bragg scattering field are assumed to be identical in Ref. [14]. On the contrary, we consider general phase functions written as $\varphi_{\pm}(z,t) = \phi(z,t) \pm \psi(z,t)$ for the field; likewise the population difference are assumed to be $w = w_0 + 2w_1 \cos[2\psi(z,t) + 2\beta_g z]$. This general consideration of the phase functions result in the demonstration that the phase modulation effects of the forward and Bragg scattering field both satisfy the general SIT chirping equation. To our best knowledge, this chirping relation for the SIT propagating through a uniformly doped nonlinear PBG structure is shown for the first time.

Although our model is more general, in contrast with the main subject of single pulse solutions in Ref. [14], we focus our studies on the exact pulse-train solutions to the Bloch-NLCMEs. Notice that the Jacobi elliptic pulse-train solutions to the Maxwell-Bloch equations for a resonance medium without PBG structure have been theoretically studied [4] and experimentally demonstrated [6]. However, our model involves considering a resonance medium whose resonant atoms embedded in a PBG structure. It is well known that a PBG structure has a forbidden band for optical energy, but the SIT provide a mechanism to make it possible that an optical pulse train can pass through the PBG medium. The pulse trains in a uniformly doped nonlinear PBG structure are given by the sinusoidal functions and have to exist with background intensity. Because the PBG medium is transparent for the SIT, such research with respect to optical pulse propagation in a doped nonlinear PBG structure has attracted much interest. It has been further suggested that a doped nonlinear PBG structure could be applied to high sensitivity optical filter, pulse reshaping devices, and optical switching devices for optical computing, optical

interconnection and optical communication system [7-14]. It is our hope that our general model can accurately estimate the associated medium parameters and the initial condition of the input optical field for designing such a device. In addition, it would be useful to study how to excite the pulse trains in a real doped PBG medium and what are the impacts of the relaxation effects on the stability of the pulse trains. These subjects would lead to practical applications of uniformly doped PBG structures in the vast area of lightwave systems.

In summary, we have established the Bloch-NLCMEs to model the SIT effect in a one-dimensional nonlinear PBG structure doped uniformly with inhomogeneously broadening two-level atoms. Our studies confirm that the Bloch-NLCMEs have exact analytic solutions related to the sinusoidal functions. Such a new type of pulse-train solution describes how the SIT evolves in a uniformly doped nonlinear PBG structure. We show that the pulse train propagating in a uniformly doped PBG structure obeys the general SIT phase modulation effect and there must be a dc term in the total intensity of the pulse train. Furthermore, because both SIT and Bragg scattering slow down the light, the pulse-train group velocity can be substantially less than the speed of light in a bare nonlinear medium. Numerical examples of the SIT pulse train in a silica-based PBG structure doped uniformly with Lorentzian line-shape two-level atoms are demonstrated. It is found that even if the carrier frequency of the pulse train is deeper inside the forbidden band, the pulse trains can propagate through the PBG structure. Namely, the SIT pulse train renders the PBG structure transparent.

This work was supported by the National Science Council, Taiwan, R.O.C. under contract NSC 89-2215-E-009-112.

REFERENCES

- [1] S. L. McCall and E. L. Hahn, Phys. Rev. Lett. **18**, 908, (1967).
- [2] J. H. Eberly, Phys. Rev. Lett. **22**, 720, (1969).
- [3] M. D. Crisp, Phys. Rev. Lett. **22**, 820, (1969).
- [4] L. Matulic and J. H. Eberly, Phys. Rev. A. **6**, 822, (1972).
- [5] M. Nakazawa, Y. Kimura, K. Kurokawa, and K. Suzuki, Phys. Rev. A. **45**, 23, (1992).
- [6] J. L. Shultz and G. J. Salamo, Phys. Rev. Lett. **78**, 855, (1997).
- [7] S. John and T. Quang, Phys. Rev. A. **54**, 4479, (1996).
- [8] S. John and T. Quang, Phys. Rev. Lett. **76**, 2484, (1996).
- [9] S. John and T. Quang, Phys. Rev. Lett. **74**, 3419, (1995).
- [10] M. Woldeyohannes and S. John, Phys. Rev. A. **60**, 5046, (1999).
- [11] A. E. Kozhokin and G. Kurizki, Phys. Rev. Lett. **74**, 5020, 1995.

- [12] A. E. Kozhokin, G. Kurizki and B. A. Malomed, Phys. Rev. Lett. **81**, 3647, 1998
- [13] M. Blaauboer, G. Kurizki and B. A. Malomed, Phys. Rev. E. **62**, R57, 2000
- [14] N. Aközbek and S. John, Phys. Rev. E. **58**, 3876, (1998).
- [15] G. P. Agrawal, *Applications of Nonlinear Fiber Optics* (Academic Press, New York, 2001).
- [16] S. Chi and S. Wen, Opt. Quant. Electron. **28**, 1351, (1996)
- [17] S. Chi, T. Y. Wang and S. Wen, Phys. Rev. A. **47**, 3371, (1993).
- [18] N. Aközbek and S. John, Phys. Rev. E. **57**, 2287, (1998).
- [19] J. Feng and F. K. Kneubühl, IEEE J. Quant. Electron. **29**, 590, (1993).
- [20] B. J. Eggleton, C. M. de Sterke and R. E. Slusher, J. Opt. Soc. Am. B. **16**, 587, (1999)
- [21] B. I. Mantsyzov, Phys. Rev. A **51**, 4939 (1995)

Ultrashort Bragg Soliton in a Fiber Bragg Grating

Sien Chi, Boren Luo and Hong-Yih Tseng

Institute of Electro-Optical Engineering, National Chiao-Tung University, Hsinchu, Taiwan, 300, R.O.C

The propagation of a nonlinear ultrashort pulse in a photonic bandgap structure is investigated by using the finite difference time domain method. The simulation results show that an ultrashort pulse near the bandgap edge can propagate through a nonlinear fiber Bragg grating, even if the broadband spectrum of this ultrashort pulse overlaps the whole forbidden band of the grating. Hence we numerically confirm that an ultrashort Bragg soliton exists beyond the low-intensity limit. It is also shown that the time delay of such an ultrashort Bragg soliton is proportional to its detuning wavelength from the exact Bragg resonance.

Introduction

Gap solitons are solitary waves propagating in a nonlinear photonic bandgap (PBG) structure [1]. The exact analytic solution to describe such a nonlinear pulse has been obtained from the nonlinear coupled-mode equations (NLCMEs). By using the multiple scale method [4], the NLCMEs can be reduced to the nonlinear Schrödinger equation (NLSE). Soliton solutions to this approximated NLSE are called Bragg solitons. Bragg solitons exist near the PBG edge and have been widely discussed both in theory [4-7] and experiment [8,9]. It has been demonstrated that a Bragg soliton can propagate through a fiber Bragg grating (FBG) [8]. The experimental results are very good agreement with the NLSE model.

One of the attractive characteristics of a Bragg soliton is the reduction of its group velocity. The experiments have shown that such a soliton-like pulse with 80-ps width can travel with the velocity as low as 70% of the light speed in an unprocessed fiber. Thus all optical buffer based on the slow propagation of a Bragg soliton is an ongoing challenge. Moreover, nonlinear compression for optical pulses by using FBGs is also an interested subject associated with the Bragg soliton propagation. Such research may result in applying solitary propagation in FBGs to practical all-optical communication system. However, to investigate the dynamics of a Bragg soliton, the models of the NLCMEs and the NLSE have the following drawbacks: (i). The NLCMEs are derived from Maxwell's equation under the slowly varying envelope approximation. This approximation renders the NLCMEs invalid to predict the characteristics of a Bragg soliton in a FBG with large index variations and arbitrarily apodized grating profile. (ii). The NLSE is derived from the NLCMEs under the low-intensity limit. This limitation restricts a Bragg soliton to a broad pulse, but for a high-speed lightwave system an ultrashort pulse is more practical and necessary.

In this paper, we use the finite difference time domain (FD-TD) method to study the nonlinear ultrashort pulse in a PBG structure. The FD-TD method can directly simulate Maxwell's equations. Hence it provides a robust simulation theory to investigate the characteristics of a Bragg soliton without any approximation. It is shown that a nonlinear ultrashort pulse near the bandgap edge still can propagate through

a FBG, even if the broad spectrum of this ultrashort pulse overlaps the whole forbidden band of the FBG. Consequently, we clarify that the existence of a Bragg soliton is not constrained by the low-intensity limit.

Simulation theory

We consider an electromagnetic field with the electric component E_z polarized along the x -axis and the magnetic component H_y polarized along the y -axis. Such an electromagnetic field propagates along the x direction in a medium, which is assumed to be non-permeable, isotropic and non-dispersive. Maxwell's curl equations for this problem are written as

$$\frac{\partial H_y}{\partial t} = \frac{1}{\mu_0} \frac{\partial E_z}{\partial x}, \quad (1)$$

$$\frac{\partial D_z}{\partial t} = \frac{\partial H_y}{\partial t}, \quad (2)$$

$$D_z = \epsilon_0 \epsilon_\infty(x) E_z + P_z^{NL}, \quad (3)$$

where μ_0 is vacuum permeability, ϵ_0 is vacuum permittivity, $\epsilon_\infty(x)$ is the relative material permittivity, D_z is the electric induced polarization including the linear and nonlinear contributions of the medium, and P_z^{NL} is the nonlinear polarization regarding the Kerr nonlinearity. On the basis of the FD-TD method, the finite difference equations for Eqs. (1) and (2) are

$$H_y \Big|_{i+1/2}^{n+1/2} = H_y \Big|_{i+1/2}^{n-1/2} + \frac{\Delta t}{\mu_0 \Delta x} (E_z \Big|_{i+1}^n - E_z \Big|_i^n), \quad (4)$$

$$D_z \Big|_i^{n+1} = D_z \Big|_i^n + \frac{\Delta t}{\Delta x} (H_y \Big|_{i+1/2}^{n+1/2} - H_y \Big|_{i-1/2}^{n+1/2}), \quad (5)$$

where Δt and Δx are the finite difference intervals in the temporal and spatial domain, respectively. The procedures of the FD-TD approach are described in the following. First Eq. (4) is used to determine $H_y \Big|_{i+1/2}^{n+1/2}$ from the previous values of $H_y \Big|_{i+1/2}^{n-1/2}$, $E_z \Big|_{i+1}^n$ and $E_z \Big|_i^n$. Second $D_z \Big|_i^{n+1}$ is determined by using Eqs. (5) from the

previous values of $D_z|_i^n$, $H_y|_{i+1/2}^{n+1/2}$ and $H_y|_{i-1/2}^{n+1/2}$. Finally the resulting $D_z|_i^{n+1}$ are substituted into Eq. (3) to determine $E_z|_i^{n+1}$ under the Newton iterative procedure:

$$E_z^{<p+1>} = \frac{D_z|_i^{n+1}}{\mathbf{e}_0[\mathbf{e}_\infty(x) + \mathbf{c}^{(3)}|E_z^{<p>}|^2]}, \quad (6)$$

where $\mathbf{c}^{(3)}$ is the third-order susceptibility, p is zero or positive integral, and $E_z^p = E_z^n$ for $p=0$.

To investigate Bragg solitons in a one-dimensional PBG medium, we consider a uniform FBG with the relative material permittivity $\mathbf{e}_\infty(x) = n(x)^2$, where

$$n(x) = n_0 + \Delta n \cos\left(\frac{2\pi x}{\Lambda}\right). \quad (7)$$

Here n_0 is the linear refractive index at the central wavelength of the electric field, Δn is the magnitude of the periodic index variations, and Λ is the grating period with respect to the Bragg wavelength \mathbf{I}_B via $\Lambda = \mathbf{I}_B / 2n_0$. It is noticed that during the FD-TD process, there is no constraint on the quantity of Δn and the apodized profile of the grating. Thus the FD-TD method is more suitable than the NLCMEs and the NLSE model to investigate the dynamics of a nonlinear pulse in a realistic rectangular waveguide grating or an apodized FBG. Such nonuniform gratings have been widely discussed for pulse compression and all-optical delay line based on the mechanisms of the Bragg soliton. Nevertheless, in the present paper, we focus our attention on how an ultrashort pulse evolves in a uniform FBG with Kerr nonlinearity, if the broad spectrum of this ultrashort pulse overlaps the whole forbidden band of the FBG.

Numerical results and discussions

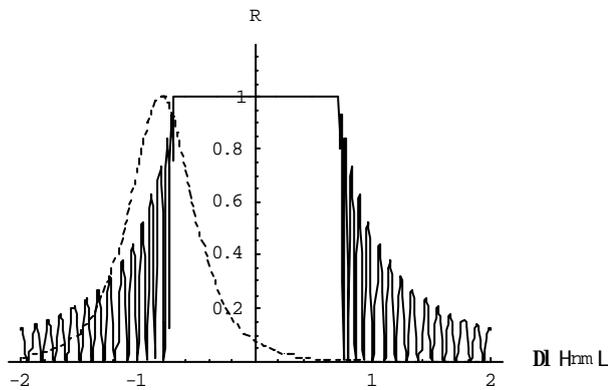


Fig. 1. The reflectivity (solid curve) of the uniform FBG and the broadband spectrum (dotted curve) of the incident pulse as functions of the wavelength detuning $\Delta \mathbf{I} = \mathbf{I} - \mathbf{I}_B$ from the exact Bragg resonance.

The solid curve in Fig.1 shows the reflectivity $R(\Delta \mathbf{I})$ of the uniform FBG in our simulation. The linear refractive index of this FBG is $n_0 = 1.5$ and the index variation is $\Delta n = 9 \times 10^{-4}$. The central wavelength of this reflectivity is $\mathbf{I}_B = 1.55 \mu\text{m}$. The dotted curve in Fig.1 shows the spectrum of the adopted incident pulse with a hyperbolic-secant pulse shape initially. The full width at half maximum (FWHM) of this pulse is assumed to be $T_f = 5.28 \text{ ps}$; likewise the central wavelength of this incident pulse is located at $\mathbf{I}_0 = 1.5492 \mu\text{m}$. Both of the FBG reflectivity and the pulse spectrum are shown as functions of the Bragg wavelength detuning $\Delta \mathbf{I} = \mathbf{I} - \mathbf{I}_B$. Furthermore, the range with $R(\Delta \mathbf{I}) = 1$ exhibits the forbidden band of such a PBG structure. It is obviously that the initial pulse spectrum exceeds the PBG edge and even overlaps the whole forbidden band. We emphasize that because of the low-intensity limit for Bragg solitons, the previously demonstrated experiments and simulations have not yet clarified the existence of a nonlinear pulse with such a broadband spectrum. We use FD-TD method to examine the dynamics of this nonlinear ultrashort pulse beyond the low-intensity limit. By choosing a uniform FD-TD space resolution $\Delta x = 50 \text{ nm}$, the numerical phase error is limited to about 3.6×10^{-5} , which is much smaller than the dispersion due to the PBG structure. Figure 2 shows the

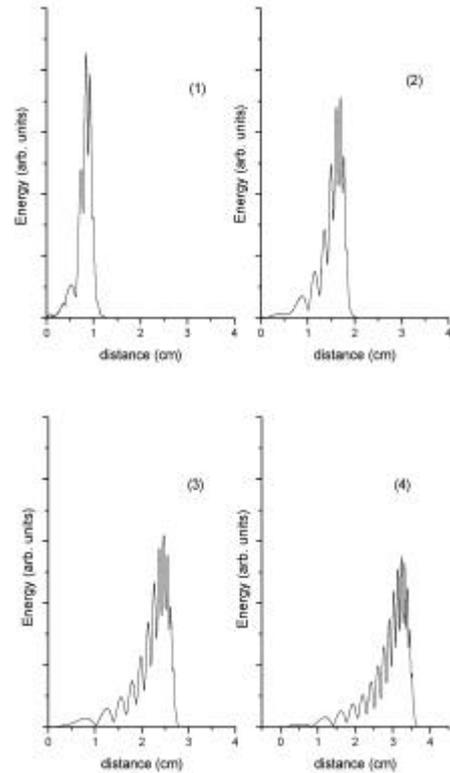


Fig. 2. Monitoring the propagation of a low-amplitude pulse in the fiber grating. The FD-TD method gives the snapshot of the propagating pulse at (1) $t=15 \text{ ps}$, (2) $t=60 \text{ ps}$, (3) $t=105 \text{ ps}$, and (4) $t=150 \text{ ps}$.

evolution of the incident pulse with low peak power $P=1.4\times 10^{-12}W$ propagating through the FBG. The Kerr coefficient of this FBG is $g=2.0\times 10^{-3}m^{-1}W^{-1}$ and the grating length is $L=38mm$. After the initial pulse is put into this FBG, Fig. 2(a), 2(b), 2(c) and 2(d) show the pulse shapes at $t=15ps$, $t=60ps$, $t=105ps$, and $t=150ps$, respectively. One can see that the shapes of this pulse are asymmetrically broadened as a consequence of its broadband spectrum. The evolution of the peak power and the spatial width of the pulse versus the propagating distance are shown in Fig. 3.

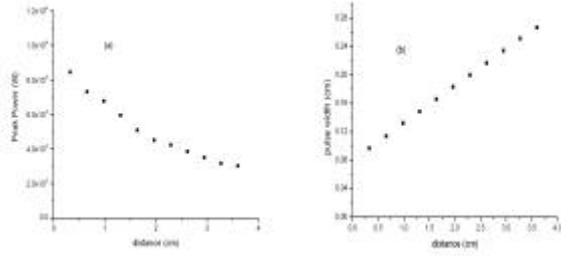


Fig. 3. (a) Peak power and (b) spatial pulse width of the low-amplitude pulse versus the propagating distance.

During the propagation, the pulse undergoes the large quadratic grating dispersion. Such a large dispersion is produced by the interference among the multi-layers of the grating. To balance this quadratic grating dispersion, we have to increase the peak power of the initial pulse.

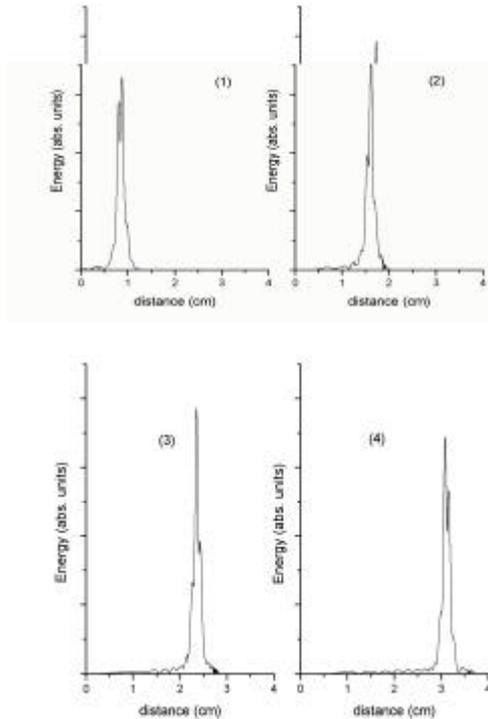


Fig. 4. Monitoring the propagation of the soliton-like pulse in the FBG. The FD-TD method gives the snapshot of the propagating pulse at (1) $t=15$ ps, (2) $t=60$ ps, (3) $t=105$ ps, and (4) $t=150$ ps.

Fig. 4 shows the evolution of the nonlinear ultrashort pulse with peak power $P=1.4\times 10^5W$. Figure 4(a), 4(b), 4(c) and 4(d) represent the pulse shapes at $t=15ps$, $t=60ps$, $t=105ps$, and $t=150ps$, respectively. It is shown that the peak power and the pulse width are almost unchanged during the propagation. Hence the balance between the nonlinearity and the quadratic grating dispersion leads to a soliton-like pulse. Figure 5 explicitly shows the evolution of the peak power and the spatial width versus the propagating distance. The numerical results show that the incident hyperbolic-secant pulse becomes quasi-stable. The pulse adjusts its amplitude and duration periodically because of the interaction between the nonlinearity and the quadratic grating dispersion. The soliton periodic L_s for such a solitary wave can be defined by the nonlinear length L_{nl} via $L_s = \pi L_{nl} / 2 = \pi / (2g \cdot P)$. Therefore the soliton-like wave propagates about 16.7 soliton periods.

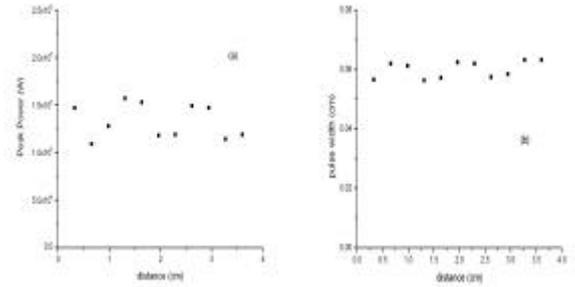


Fig. 5. (a) Peak power and (b) spatial pulse width of the soliton-like pulse versus the propagating distance. It is shown that the pulse adjusts its amplitude and duration periodically because of the interaction between the nonlinearity and the quadratic grating dispersion.

Another notable characteristic of this solitary wave is its propagating delay with respect to the propagating time of the light in an unprocessed fiber. For the above hyperbolic-secant pulse with carrier frequency $\omega_0 = 1.5492 \mu m$, the delay after propagating through the grating with length $L=38mm$ is $42ps$. This delay corresponds to the soliton's group velocity as low as 72% of the light speed in an unprocessed fiber. The group velocity of our adopted ultrashort pulse is very close to that of the Bragg solitons demonstrated previously in the experiment [8]. Figure 6 further displays the time delay versus the carrier wavelength of the ultrashort Bragg soliton. One can see that the delay is linearly proportional to the Bragg detuning wavelength. Note that both of the NLCMEs and the NLSE model cannot predict such a relation between the time delay and the carrier wavelength detuning of an ultrashort Bragg soliton. Consequently, it would be useful to apply the FD-TD method to estimate the group velocity of an ultrashort Bragg soliton, especially for designing an all-optical buffer in practical high-speed communication systems.

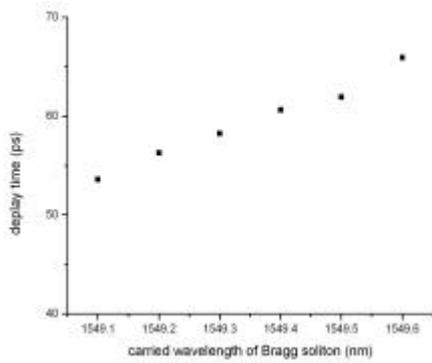


Fig. 6. Time delay versus different carried wavelength of the ultrashort Bragg soliton.

Conclusion

We have applied the FD-TD method to investigate the nonlinear ultrashort pulse in a fiber Bragg grating. The FD-TD method can directly simulate Maxwell's equation and inherently computes the bi-directional electromagnetic field without using any approximation. As a result, our study numerically confirms that the existence of a Bragg soliton is not constrained by the low-intensity limit. An ultrashort Bragg soliton still could propagate through a nonlinear PBG structure, even if its broadband spectrum overlaps the forbidden gap of the PBG medium. The propagating dynamics which have not yet been clarified by the NLCMEs and the NLSE model are explicitly shown on the basis of the FD-TD method. Furthermore, the FD-TD method shows that the time delay of an ultrashort Bragg soliton is linearly proportional to the Bragg detuning wavelength. It would be useful to apply the FD-TD method to design an all-optical delay line in a realistic high-speed telecommunication system.

Acknowledgement

This work was supported by the National Science Council, Taiwan, R.O.C. under contract NSC 89-2215-E-009-112.

References

1. Wei Chen and D. L. Mills, *Phys. Rev. Lett.* **58**, 160 (1987)
2. S. M. de Sterke and J. E. Sipe, in *progress in Optics*, edited by E. Wolf (North-Holland, Amsterdam, 1994), Vol. XXXIII, pp.203-260
3. C. Martijn de Sterke and J. E. Sipe, *Phys. Rev. A.* **38**, 5149 (1988)
4. C. Martijn de Sterke and J. E. Sipe, *Phys. Rev. A.* **39**, 5163 (1989)
5. A. B. Aceves and S. Wabnitz, *Phys. Lett. A* **141**, 37 (1989)
6. D. N. Christodoulides and R. I. Joseph, *Phys. Rev. Lett.* **62**, 1746 (1989)
7. C. Martijn de Steke and B. J. Eggleton, *Phys. Rev. E* **59**, 1267 (1999)
8. B. J. Eggleton, R. E. Slusher and C. Martijn de Sterke, *Phys. Rev. Lett.* **76**, 1627 (1996)
9. B. J. Eggleton, C. Martijn de Steke, *J. Opt. Am. B* **16**, 587 (1999)